PEOPLE'S DEMOCRATIC REPUBLIC OF ALGERIA
Ministry of Higher Education and Scientific Research
University of Mohamed El Bachir El Ibrahimi
Faculty of Science and Technology

DOCTORAL THESIS

Presented to obtain the degree of **DOCTOR**

In : Electronics

Specialty : Embedded Systems

By : Tiaiba Hichame

Topic

Conception d'algorithmes de commande pour des robots portables de type exosquelettes

Publicly defended, on **29/09/2024**, before a jury composed of :

Mr.	BEKKOUCHE Tewfik	Associate Professor/A	at UBBA	President
Mr.	DAACHI Mohamed El Hossine	Associate Professor/A	at UBBA	Thesis Director
Mr.	MADANI Tarek	Associate Professor/HDR	at UPEC-France	Thesis Co-Director
Mr.	AMARDJIA Noureddine	Professor	at UFAS	Examinator
Mr.	BOUGUEZEL Saad	Professor	at UFAS	Examinator
Mr.	LATOUI Abdelhakim	Associate Professor/A	at UBBA	Examinator

Abstract In this doctoral thesis, we have developed a novel adaptive control approach based on higher-order sliding modes, coupled with the Particle Swarm Optimization (PSO) algorithm. This approach is particularly well-suited for nonlinear systems, such as exoskeletons, where operating conditions can vary significantly depending on the user and the environment. The key innovation lies in the integration of the PSO algorithm for real-time adaptation of controller parameters. The combination of higher-order sliding modes with PSO offers a robust solution, ensuring optimal stability while adjusting to the fluctuations and uncertainties inherent in the interaction between the robotic system and the user. Special attention was given to demonstrating closed-loop control stability, in the Lyapunov sense, which guarantees the system's convergence to a stable behavior. To assess the effectiveness of our approach, tests were conducted first in simulation and then experimentally, involving two healthy subjects equipped with the ULEL exoskeleton available at LISSI laboratory of the University Paris-Est Créteil. The results are highly promising, highlighting a significant improvement in motion accuracy, adaptability to varying forces, and user comfort.

Résumé Dans cette thèse de doctorat, nous avons développé une nouvelle approche de commande adaptative s'appuyant sur des modes glissants d'ordre supérieur, couplée à l'algorithme d'optimisation PSO (Particle Swarm Optimization). Cette approche est particulièrement bien adaptée aux systèmes non linéaires, tels que les exosquelettes, où les conditions d'utilisation peuvent varier considérablement en fonction de l'utilisateur et de l'environnement. L'innovation majeure réside dans l'intégration de l'algorithme PSO pour une adaptation en temps réel des paramètres de commande. L'association des modes glissants d'ordre supérieur avec le PSO offre une solution robuste, garantissant une stabilité optimale tout en s'ajustant aux fluctuations et incertitudes inhérentes à l'interaction entre le système robotique et l'utilisateur. Nous avons accordé une attention particulière à la démonstration de la stabilité en boucle fermée de la commande, au sens de Lyapunov, qui assure la convergence du système vers un comportement stable. Pour évaluer l'efficacité de notre approche, des tests ont été réalisés d'abord en simulation puis expérimentalement, impliquant deux sujets sains équipés de l'exosquelette ULEL disponible au laboratoire LISSI de l'université Paris-Est Créteil. Les résultats obtenus sont très prometteurs, mettant en évidence une amélioration significative en matière de précision des mouvements, d'adaptabilité aux variations de forces, et de confort pour les utilisateurs.

Contents

List of Figures

List of Tables

Acknowledgements & Dedication

I would like to express my sincerest gratitude to Allah for bestowing upon me the faith, strength, courage, and patience to complete this thesis. I dedicate this modest work and my profound gratitude to my parents, my siblings, and my entire family for their unwavering encouragement and prayers, which have enabled me to achieve this modest accomplishment. I am immensely grateful for the confidence they have placed in me.

I would like to express my appreciation to my supervisor, Dr. M.E. Daachi from Bordj Bou Arreridj University, for his unwavering confidence in me, his persistent guidance, his modesty, his invaluable advice, and his constructive feedback, all of which significantly contributed to the successful completion of this research.

My heartiest thanks and gratitude to my co-supervisor Dr. T. Madani from Paris Est Créteil University in France for his invaluable guidance, support, and patience throughout the completion of this thesis. I also extend great respect and thanks to LISSI laboratory in france for adopting the testing and validation of my research. Likewise, i'm indebted to all those who provided assistance and feedback, which proved invaluable in enhancing the quality of this manuscript.

I would like to extend my sincerest gratitude to my distinguished examiners, Professor AMARDJIA Noureddine, Professor BOUGUEZEL Saad, Dr. LATOUI Abdelhakim, and Dr. BEKKOUCHE Tewfik. Their insightful feedback and expert guidance have significantly contributed to the quality and completion of this thesis. I am truly honored to have had the opportunity to be evaluated by such experts.

May God's blessings and peace be upon Mohammad and his family and all companions.

Introduction:

In the 21st century, the field of exoskeleton robotics has advanced rapidly in various applications, including healthcare, military, industry, and consumer sectors.

Robots have been identified as a possible way to improve and automate patients' access to rehabilitation therapy, as well as provide new tools for therapists. In contrast to conventional techniques, which require significant time and energy and often yield unsatisfactory results, robot-assisted rehabilitation offers a promising alternative. In the current era, the prevalence of stroke patients has reached a staggering number, with over 13.7 million new cases recorded annually. Conventional rehabilitation techniques have proven inadequate for effectively treating all patients, prompting the emergence of exoskeleton robots that can assist disabled individuals in regaining control of their limbs [1–5]. These robots have also been utilized in military domains and other fields.

Robots are mechatronic devices designed to automatically perform tasks that imitate or reproduce human actions within a particular area. Consequently, they have a long history of association with humans, with the first such devices being developed in the 1960s and 1970s. Although their cost is high, they are intended to replace or assist human operators in repetitive, challenging, or dangerous tasks. The evolution of electronics and computing has enabled the development of robots that are more precise, faster, and have a better autonomy, which has facilitated greater data exchange, as exemplified by teleoperation robotics. Moreover, the advent of wearable robots has prompted investigations into aspects of physical interaction.

In general, two types of wearable robots can be distinguished: prostheses and exoskeletons. In contrast to prostheses, which are designed to replace a missing body part, exoskeletons are intended to operate in conjunction with the human limb. The joint axes of these devices correspond to those of the wearer's limb, imitating its structure. Exoskeletons have a number of potential applications, including the enhancement of power in military and rescue contexts, the provision of diagnostic and technical assistance to individuals with disabilities or impaired mobility, industrial assistance and manufacturing, and the facilitation of physical therapy [6–8], which encompasses the rehabilitation of motor functions. Since our research involved an upper limb exoskeleton, this thesis primarily examines similar exoskeletons and their applications.

The primary treatment for disabilities resulting from a stroke is rehabilitation therapy, which facilitates the recovery of voluntary movements and the relearning of activities of daily living [9]. Stroke is the leading cause of serious and long-term disability [10]. The location and severity of the lesion determine whether a stroke results in partial or total paralysis [11]. As the number of disabled patients continues to grow, the challenge of providing appropriate treatment will become increasingly challenging and costly. As an

effective solution, the utilization of exoskeletons enables the fulfillment of this expanding demand and can enhance the well-being of patients afflicted with such conditions. Having a kinematic profile analogous to that of the human limb, exoskeletons can facilitate a sustained and comprehensive rehabilitation over extended periods and reduced expenses [12]. Additionally, exoskeletons can furnish data and measurements that could be employed to assess the patient's recovery.

This manuscript is organized into four chapters, in addition to an introduction and a conclusion.

The first chapter offers a comprehensive overview of exoskeleton robots, a class of wearable robotic devices designed to enhance, augment, or support human physical abilities. It provides a historical overview of exoskeletons, examines their diverse applications, and discusses the technological advancements that have contributed to their development. The applications discussed include healthcare and rehabilitation, industrial assistance, military and defense, and assistance in daily living activities. The chapter outlines the fundamental concepts, components, and the biomechanics, materials science, and robotics principles underlying exoskeleton robots.

The second chapter is dedicated to the geometric, kinematic, and dynamic modeling of the Upper Limb Exoskeleton of LISSI (ULEL), which serves as the experimental platform for this thesis. It provides a detailed account of the mechanical properties and the innovative actuation and transmission system of ULEL. Furthermore, it explores the modeling of ULEL using the modified Denavit-Hartenberg (DH) method and examines the various control strategies employed in limb rehabilitation, including assistive and resistive control strategies.

The third chapter provides a comprehensive account of the Particle Swarm Optimization (PSO) algorithm, an optimization technique inspired by the social behavior of birds and fish. It explains the initialization phase, velocity and position updates, fitness evaluation, and termination conditions of the PSO algorithm. Furthermore, it examines the significance of various parameters in the PSO algorithm, challenges such as scalability and memory requirements, and future directions for research and application of PSO in fields like image processing, computational biology, and recommender systems.

The final chapter presents the main contributions of this research, which focus on the development of a real-time adaptive Super Twisting Sliding Mode Control (ST-SMC) algorithm enhanced by PSO. This novel approach addresses limitations in existing exoskeleton control methods, such as offline tuning and heavy calculation. The stability and effectiveness of the proposed controller are validated through simulations and real time experiments, demonstrating improved performance and robustness in controlling nonlinear systems like exoskeletons.

The manuscript is concluded with a general conclusion and perspectives for future work.

Chapter 1

Exoskeleton robots: State of the art

1.1 Introduction:

Exoskeletons, are a wearable robotic devices designed to enhance, augment, or support the physical abilities of the human body. These devices are typically worn externally and interact with the user's body to provide assistance, correction, and rehabilitation.

Exoskeletons have been introduced the first time in 1960s, where the first successful developed prototype which called Hardiman appeared [13].It was made for military purposes to strengthen the physical abilities of the soldiers. In the last couple decades, exoskeletons have been utilized and revolutionized the field of daily living activities and rehabilitation. Where it gained the potential of being a permanent solution for physically disabled people [14], neuromuscular impairment [6, 7], post stroke rehabilitation [15, 16], and power amplification in an industrial environment [8].

Exoskeleton robots have diverse applications across various fields [17], such:

- *Healthcare and Rehabilitation*: Assisting individuals with mobility impairments due to neurological disorders, spinal cord injuries, stroke, and other conditions in regaining and improving their physical abilities [18–22].
- *Industrial assistance and manufacturing:* augmenting human strength and endurance to reduce the risk of injury and increase productivity during physically demanding tasks such as lifting, carrying, or repetitive motions [23–25].
- *Military and defense:* Providing soldiers and first responders with enhanced strength, maneuverability, and force in hazardous environments [26].
- *Assistance in activities of daily living:* Supporting elderly individuals or those with mobility limitations in performing everyday tasks such as walking, standing, and reaching distant locations [27].

The objective of this chapter is to provide an overview of exoskeleton robots and their application. Starting with the fundamental concepts and different components of an exoskeleton. Then classification and types of the exoskeletons are presented. After that, various applications and use cases of this type of robot are given. Finally, the studied exoskeleton robot is described in detail, followed by a discussion of the challenges and future directions.

1.2 Fundamental concepts and components:

Exoskeletons are remarkable creations of engineering, designed to enhance human performance and augment physical capabilities. The fundamental principles underlying their design and operation encompass biomechanics, materials science, robotics, and human-machine interaction. These principles are outlined in the following points:

1. Biomechanics [28]: Exoskeletons have been designed to imitate the natural movements of the human body. An understanding of biomechanics enables engineers to create structures and joints that move in a manner that is complementary to human motion, which in turn reduces fatigue and strain.

2. Materials Science [29]: The materials used in exoskeleton construction are crucial for strength, flexibility, and weight. Lightweight yet durable materials like carbon fiber, titanium, and advanced plastics are often used to ensure the exoskeleton is both robust and comfortable for the user.

3. Robotics: Exoskeletons are robotic devices that incorporate actuators, sensors, and controllers in order to assist or amplify human movement. The function of the actuators is to provide the power to move the exoskeleton, while the sensors gather data on the user's movements and intentions in real-time. This enables the exoskeleton to make real-time adjustments and provide real-time feedback.

4. Human-Machine Interaction [30, 31]: In order for an exoskeleton to function effectively, it must be designed to seamlessly integrate with the user's body and movements. This integration is contingent upon a number of factors, including ergonomics, the design of the user interface and control algorithms, all of which must be carefully considered in order to ensure that the exoskeleton responds intuitively to the user's commands and movements.

5. Power Source [32]: The operation of exoskeletons necessitates the availability of a power source. This can be batteries, hydraulic systems, or even human-generated power, such as through kinetic energy harvesting [33]. It is therefore essential to implement an efficient power management system in order to prolong battery life and ensure the exoskeleton remains operational for extended periods.

6. Customization and Adaptability [34]: Exoskeletons frequently necessitate adjustments to accommodate users of diverse sizes and physical abilities. The availability of customized options facilitates a more accommodating fit and optimal performance for each individual user.

Adherence to these principles permits exoskeleton designers to create devices that augment human strength, endurance, and mobility, while assuring safety and usability. As technology progresses and our comprehension of human-machine interaction deepens, these principles are subject to continuous evolution.

1.2.1 Key components:

Exoskeleton robots feature a number of key components and characteristics that set them apart from other types of robots. These include

- **Frame and structure** [35–37]: An exoskeleton is a device comprising a rigid or semi-rigid frame that encircles specific body parts, such as the upper or lower limbs or the torso. This frame serves to provide structural support and to act as a platform for mounting additional components

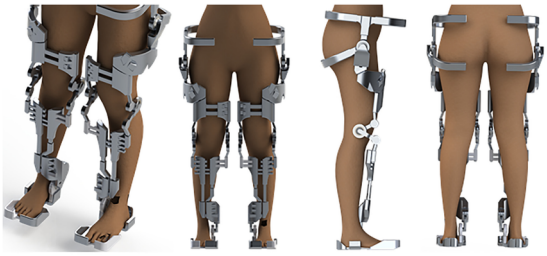

Figure 1.1: Lower limb exoskeleton frame [36].

- **Actuators and joints** [35, 38]: Actuators, which frequently take the form of motors or pneumatic systems, are integrated into the exoskeleton with the objective of providing mechanical assistance and facilitating movement at the joints. These actuators replicate the functionality of human muscles, enabling the user to amplify or augment their movements.

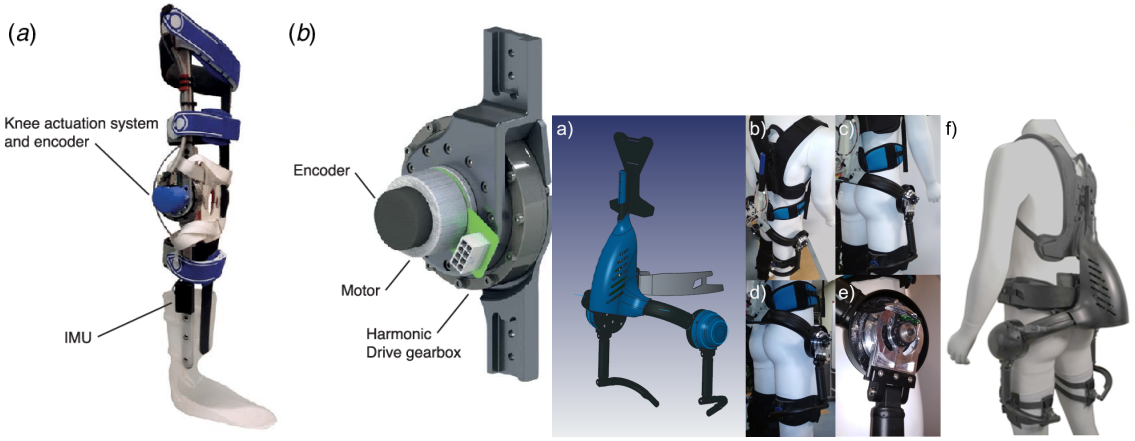

Figure 1.2: Exoskeleton actuators and joints [39, 40].

- **Sensors and control systems**: Exoskeletons are equipped with sensors that are able to detect and transform the movements and intentions of users into a exploitable signal in real time. These sensors provide feedback to sophisticated control systems, which in turn adjust the exoskeleton's behavior to optimize performance while ensuring the safety and comfort of the user [41, 42].

Figure 1.3: EMG sensors used for an exoskeleton [43].

- **Power source**: The operation of exoskeletons necessitates the presence of a power source, which is responsible for the functioning of their actuators, sensors, and control systems. This power source may take the form of batteries, pneumatic systems, or other energy storage devices, contingent upon the design and intended use of the exoskeleton.

1.3 Types and classification:

Exoskeletons can be classified based on various criteria, including their application, design, and control mechanism. Here are some common types:

1.3.1 Powered exoskeletons vs passive exoskeletons:

Powered exoskeletons are devices that utilize motors or actuators to enhance the strength and mobility of the wearer, enabling tasks such as heavy lifting and providing support during movement [44–46]. In contrast, passive exoskeletons lack active energy sources and rely on mechanical structures and springs for support as stated in [47, 48]. While the capabilities of powered exoskeletons are well suited to tasks that require a high level of force, passive exoskeletons are often preferred for their inherent simplicity and reliability, particularly in industrial settings.

1.3.2 Stationary exoskeletons vs mobile exoskeletons:

Stationary exoskeletons are designed for fixed-location use, providing targeted support for specific tasks or aiding in rehabilitation exercises. In contrast, mobile exoskeletons offer portability, thereby allowing users freedom of movement [49]. These devices have applications in a number of fields, including military operations, healthcare, and assistive technology. Their primary focus is on enhancing mobility and versatility.

1.3.3 Medical exoskeletons vs industrial exoskeletons:

Medical exoskeletons are designed for specific medical applications, such as assisting in rehabilitation, providing mobility for individuals with disabilities, and supporting stroke patients as exemplified in [50]. In contrast, industrial exoskeletons are intended for use in repetitive, heavy-duty tasks in industrial environments, including lifting heavy loads and reducing fatigue to prevent injuries among workers [51].

1.3.4 Full-body exoskeletons vs partial exoskeletons:

Full-body exoskeletons encompass a substantial portion of the wearer's body, offering comprehensive support to multiple joints and muscle groups. These exoskeletons are well-suited to tasks requiring substantial physical exertion , an example of robot designed for elderly people is described in [52]. In contrast, partial exoskeletons are designed to provide targeted support for specific areas of the body, enhancing task performance and addressing mobility challenges. In contrast to full-body exoskeletons, partial exoskeletons are often more lightweight and agile.

1.3.5 Hybrid exoskeletons:

A hybrid exoskeleton combines features from both powered and passive designs [53, 54]. These mechanical structures are combined with powered actuators. By striking a balance between the assistance provided, the weight of the system, and the complexity of the design, hybrid exoskeletons offer versatile solutions that can be adapted to a variety of tasks and environments. The strengths of both approaches are leveraged to optimize functionality and user experience.

By considering the aforementioned classification criteria, it becomes possible for researchers and developers to design exoskeletons tailored to specific applications and user needs. These can be used in various domains, including healthcare, industry, and beyond.

1.4 Application and use cases:

It is evident that exoskeleton robots have the potential to revolutionize a multitude of applications within a diverse array of disciplines. These robots have the capacity to enhance the capabilities of humans, augment physical strength, and facilitate rehabilitation and daily tasks. In addition to the description of exoskeleton applications provided in the introductory section, further detail and illustrative examples of each application are presented below.

1.4.1 Medical rehabilitation and mobility assistance:

Exoskeletons are proving to be a revolutionary technology in the field of rehabilitation, offering individuals with mobility impairments a new avenue for restoring mobility and enabling them to regain full control of their limbs. This technology has been successfully employed in the treatment of spinal cord injuries and other disabilities, enabling patients

to walk again. One noteworthy example is the ReWalk exoskeleton, which has been successfully utilized by individuals with spinal cord injuries to regain mobility and enhance their quality of life [55, 56]. Similarly, the Ekso GT exoskeleton has been employed in a multitude of rehabilitation centers worldwide to assist patients with stroke or spinal cord injuries in regaining mobility and independence [57].

Indeed, the existing rehabilitation therapies can be classified into three distinct modes: assistive, corrective and resistive [58].

Assistive rehabilitation:

The objective of this mode of operation is to assist the patient in performing movements that he is unable to do independently. This mode can be further subdivided into the following categories:

- *Passive:* In this mode, the subject remains completely passive during movement while the robot drives the patient's limb during rehabilitation exercises. The system generally operates in simple position control. This mode of operation is particularly useful in the initial phase of the rehabilitation process.

- *Assistance as needed:* In that scenario, the patient initiates the movement, and the robot is there to assist, guide, and complete the movement. This mode of therapy is employed in rehabilitation phases where the patient has partially recovered his ability to move.

- *Active:* In contrast to passive and assistive modes, active control is not intended for rehabilitation but is frequently used for diagnostic and evaluation purposes. In general, there is a tendency to favor control strategies that provide only the minimum assistance necessary for the subject.

Corrective rehabilitation:

In this mode, the subject is made aware of the movement and the robot attempts to rectify it or compel it to perform the gesture with a specific articular configuration, or solely utilizing certain joints or muscle groups. This mode can be employed as a second phase of rehabilitation in order to enhance the patient's ability to perform a given task.

Resistive rehabilitation:

The objective is to make the task more challenging to complete. In this instance, the robot applies forces that are in opposition to the desired movement, with the intention of encouraging the patient to exert greater effort during the movement.

1.4.2 Augmentation of human performance in industrial settings:

In industrial settings, exoskeletons are designed to be worn by the user as a wearable device that serves to augment human performance, primarily by reducing physical strain and enhancing efficiency. These exoskeletons typically consist of an external framework, often made of lightweight materials such as carbon fiber or aluminum. This framework is worn by the users over their clothing. They are employed in a variety of industries where workers are required to lift heavy objects or perform repetitive tasks. The use of exoskeletons has been shown to reduce the risk of injury to workers and to increase productivity. For example, Hyundai's wearable robot [Hyundai motor leads personal mobility revolution with advanced wearable robots] is utilized in their manufacturing facilities to assist workers in lifting heavy objects, thereby reducing the physical strain on the workers' bodies, and preventing occupational injuries. Further illustrative examples may be found in [59], where the majority of exoskeleton types are cataloged.

The following description outlines the ways in which exoskeletons improve human performance in industrial settings.

Reduced physical strain: One of the most significant benefits associated with the utilization of exoskeletons is the capacity to diminish the physical strain experienced by the wearer. These devices provide mechanical assistance to specific body regions, such as the arms, legs, and back, thus reducing the load on muscle and joints during repetitive or strenuous tasks. This can assist in the prevention of fatigue, muscle strain, and the risk of musculoskeletal disorders.

Increased strength and endurance: Exoskeletons may be utilized to enhance the strength and endurance of the wearer by providing assistance or amplification of their movements. Powered exoskeletons, equipped with motors or pneumatic systems, can provide additional force to lift heavy objects or maintain prolonged postures, thereby enabling workers to perform tasks that would otherwise be physically demanding or tiring. This can result in increased productivity and efficiency.

Improved ergonomics: The promotion of proper posture and alignment through the use of exoskeleton technology improves ergonomic conditions in industrial settings. By maintaining neutral joint positions and distributing loads more evenly across the body, exoskeleton use reduces the risk of ergonomic injuries caused by awkward postures or repetitive movements. Improved ergonomics can result in greater comfort and lower rates of work-related injuries.

Improved safety: Exoskeletons contribute to enhanced occupational safety and health by reducing the probability of accidents and injuries. They offer stability and assistance when lifting or transporting bulky objects, thus reducing the risk of strain injuries, slips, and other accidents. Additionally, some exoskeletons are furnished with sensors and feedback systems which notify the users of potential dangers or suboptimal lifting techniques. This further improves safety in industrial settings.

1.4.3 Military applications:

In the context of military combat, exoskeletons offer enhanced strength, endurance, and protection for the individual soldier. They can assist in the transportation of heavy loads over long distances, thereby reducing fatigue and increasing operational effectiveness. The U.S. military's Tactical Assault Light Operator Suit (TALOS) project is aimed at developing an advanced exoskeleton system to provide the soldier with improved protection and mobility in combat situations. A brief overview of the military applications is shown below.

Enhanced Strength and Endurance: Exoskeletal devices have the potential to enhance the physical capabilities of soldiers, enabling them to transport heavier loads over longer distances with reduced fatigue. Powered exoskeletons that incorporate motors or hydraulic systems offer assistance during various forms of mobility, such as walking, running, or lifting. This can enhance the ability of the soldier to traverse difficult terrain and perform demanding tasks more effectively.

For instance, Onyx, created by Lockheed Martin, is a small exoskeleton that resembles a knee brace and covers the entire leg Figure 1.4. This suit's advantage is that it allows users to perform repetitive motions that they are already capable of, but with less strain on their musculoskeletal system. It is focused on knee-intensive activities such as climbing

and descending stairs, hills, and harsh environments. The Onyx weighs only 20 pounds, including its battery, rendering it suitable for use in military applications [60, 61].

Figure 1.4: Onyx exoskeleton robot.

Load Carriage and Logistics Support: The primary military application of exoskeletons is load-carriage support. During missions, soldiers frequently carry heavy equipment, weapons, and supplies, which can lead to fatigue and a decline in mobility. Exoskeletons distribute the weight of these loads more evenly across the body, providing mechanical assistance that facilitates the transportation of soldiers' gear while maintaining their mobility and agility.

For example, the Raytheon XOS-2 exoskeleton employs high-pressure hydraulics to enable the user to lift heavy objects at a ratio of 17:1. This means that the user experiences a 17-lb load when in fact the object being lifted weighs only 1 lb. The XOS-2 represents a significant advancement over the XOS-1, with notable improvements in energy efficiency. The exoskeleton itself weighs approximately 95 kg, which is considerably more than most other suits. This is due to its large size and the fact that it enhances both the lower and upper body [60, 62].

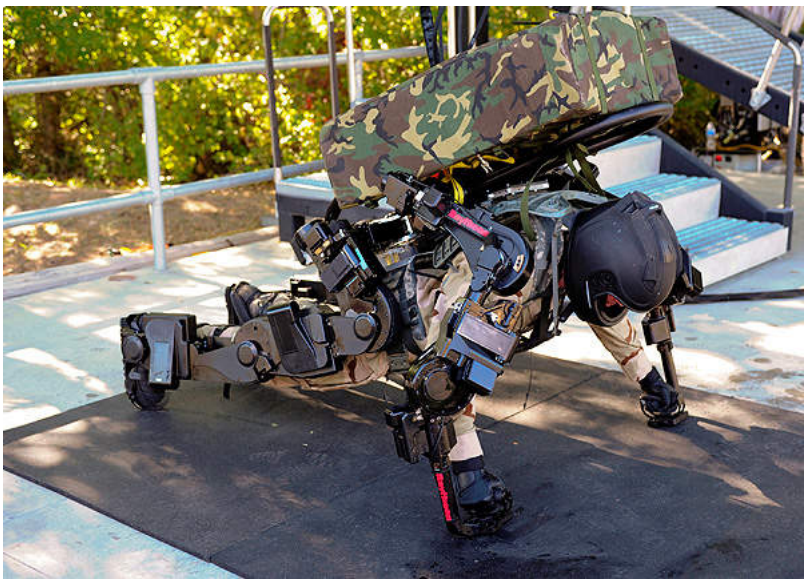

Figure 1.5: XOS-2 Exoskeleton robot

Tactical Mobility and Maneuverability: Exoskeletons enhance the tactical mobility and maneuverability of soldiers in various combat scenarios. Lightweight exoskeletons designed for agility and speed enable soldiers to move more rapidly and effectively across rugged terrain and engage enemy targets with greater efficiency. By improving a soldier's ability to traverse challenging environments and respond rapidly to changing threats, such Mawashi Uprise Tactical Exoskeleton [63, 64], exoskeletons have a positive impact on overall military operations.

Figure 1.6: Mawashi uprise tactical exoskeleton robot

Specialized Applications and Mission Support: Exoskeletons can be designed to meet the specific requirements of different military roles and missions. Specialized exoskeletons may be created for specific tasks, such as reconnaissance, urban combat, combat engineering, medical evacuation, or other specialized operations. These exoskeletons incorporate features such as stealth capabilities, integrated communication systems, or mod-

ular attachments to support mission objectives and enhance soldier survivability in diverse operational environments.

1.4.4 Assistive devices for elderly care:

Exoskeletons are currently being explored as potential assistive devices in the field of elderly care. Their objective is to help seniors maintain their independence and perform daily activities with greater ease. The efficacy of exoskeletons like the HAL (Hybrid Assistive Limb) Figure 1.7 has been evaluated in elderly care facilities, with promising results [65]. These devices have been shown to enhance mobility and reduce the risk of falls among older adults. For further details, please refer to [66], which provides a comprehensive overview of the state of the art in lower limb exoskeletons for elderly assistance.

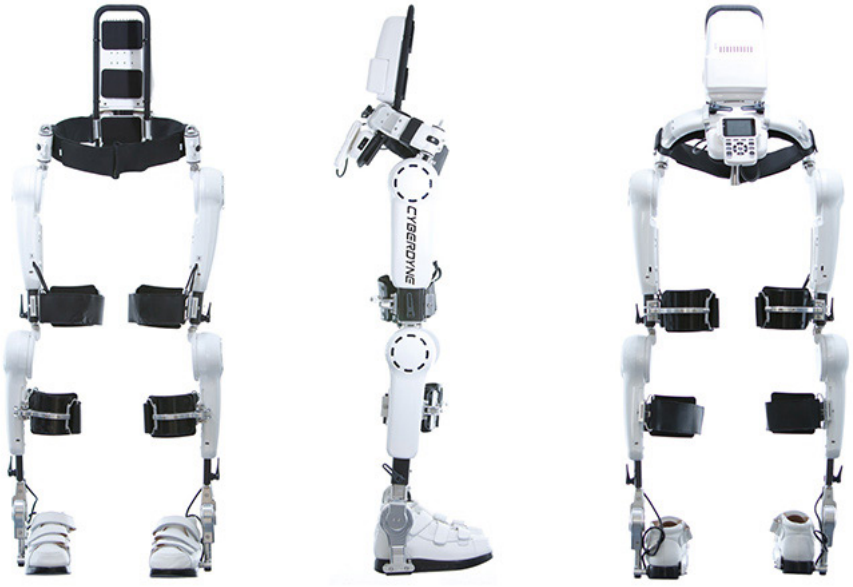

Figure 1.7: HAL exoskeleton.

1.5 Studied case exoskeleton:

The system under consideration in this study is the exoskeleton ULEL , which was specifically designed by the RB3D[1] company for the LISSI[2] Laboratory of the University Paris-Est Créteil in France. ULEL is designed with three active degrees of freedom (DoF) to be worn on the lateral side of the upper limb and is intended to provide effective rehabilitation for shoulder (flexion/extension), elbow (elbow/extension), and wrist (flexion/extension) movements. More details about ULEL, including geometric, kinematic, and dynamic models are presented in Chapter 2.

[1] www.rb3d.com

[2] Laboratoire Images, Signaux et Systèmes Intelligent, Paris - France

Remarque: Since the parameters and characteristics of the ULEL exoskeleton have been identified previously by [58], this work is based on the obtained results and can be considered as a follow-up of the that research.

Figure 1.8: ULEL Exoskeleton robot.

1.6 Challenges and future directions:

Exoskeleton technology is confronted with a number of significant challenges, including high costs, bulky designs, complex control systems, and variable user acceptance. The expense of manufacturing exoskeletons restricts accessibility, while their weight and cumbersome structures can induce discomfort and limit mobility. Moreover, intricate control algorithms must accurately interpret user movements, posing technical hurdles and increasing the risk of malfunction. Furthermore, social perceptions and ergonomic concerns may also affect the extent to which exoskeletons are accepted, which could hinder their widespread adoption across various industries and applications.

In order to overcome these difficulties, current research activities and emerging trends are driving innovation in exoskeleton technology. Efforts have been made towards the development of lightweight materials and compact designs, with the intention of relieving the burden placed on users and improving comfort. Furthermore, advances have been made in terms of sensing technologies and control algorithms, with the objective of enhancing the responsiveness and adaptability of exoskeletons for example by using machine learning technology [67–69], this will enable more intuitive interaction with users. In addition, efforts to reduce manufacturing costs and streamline production processes are ongoing, with the aim of making exoskeletons more economically feasible and accessible to a wider audience [70].

In the future, exoskeleton technology may undergo significant developments that could revolutionize human augmentation. Innovations such as soft exosuits [71], neuro-prosthetics [72], and personalized designs may facilitate more seamless integration with the human body and enhanced user experiences. By leveraging multidisciplinary collaboration and bio-inspired approaches [73], researchers may further optimize the performance and functionality of exoskeletons, paving the way for transformative applications in healthcare, industry, and beyond.

1.7 Conclusion:

This chapter provides a comprehensive overview of exoskeleton robot technology, illuminating its current status and future prospects. The fundamental concepts and components of exoskeletons have been explored in detail, revealing the complexity behind their design and operation. The key components of exoskeletons that are essential for functionality have been analyzed, thus making clear their vital role in the system. Moreover, different types of exoskeletons have been classified, demonstrating a diverse range of designs customized to address various user needs and application domains. The practical applications and use cases of exoskeletons across diverse sectors have been examined and accompanied by real-world examples to illustrate the technology's versatility and impact. Furthermore, a specific exoskeleton called ULEL designed for upper limb rehabilitation, has been presented in brief. Finally, the current research ideas and directions have been presented, as well as potential future improvements and innovations in exoskeleton technology. The following chapter will expand upon the modeling of an upper limb exoskeleton robot.

Chapter 2

Upper limb exoskeleton modeling

2.1 Introduction:

Exoskeleton modeling serves as the fundamental basis for understanding, optimizing, and enhancing the capabilities of these wearable robotic systems. This introductory section provides a framework for our subsequent discussions, emphasizing the importance of exoskeleton modeling in the context of human augmentation and assistive technologies, specifically limb rehabilitation. An in-depth examination of the theoretical underpinnings and practical applications of exoskeleton modeling is provided, laying the foundation for future advancements in human augmentation technologies. The objective of this chapter is to comprehensively explore the modeling aspects of exoskeleton robots, with a primary focus on the ULEL exoskeleton designed for upper limb rehabilitation. We begin with an explanation of the fundamental concepts in exoskeleton modeling, including geometric, kinematic, and dynamic aspects. This is followed by a real-world example of modeling an exoskeleton.

In conclusion, readers will gain a precise understanding of the theoretical foundations, practical applications, and challenges associated with modeling exoskeletons, particularly within the context of the ULEL exoskeleton.

2.2 Kinematics and dynamics of exoskeletons:

2.2.1 Upper limb anatomy: A comprehensive overview:

The upper limb is a term used to describe the upper extremity, which comprises three primary segments: the arm, forearm, and hand. Each of these segments plays an essential role in various daily activities and movements. This section provides an overview of the anatomical elements within each segment, along with an explanation of their functional significance based on

a. The shoulder:

The shoulder joint represents the most mobile of all human joints and serves as the pivotal joint connecting the upper limb to the trunk (or also called Turso). The shoulder complex, which is composed of the clavicle (or collarbone), the scapula (or shoulder blade), and the humerus (or upper arm bone), offers three DoF, which facilitate flexion/extension, adduction/abduction, and axial rotations of the upper limb.

b. The elbow:

The elbow is the intermediary articulation between the upper arm and the forearm, playing a critical role in the mechanical integration of these segments. The elbow joint is composed of the humerus, radius, and ulna and enables two primary functions, namely flexion/extension and pronation/supination. This articulation provides two DoF, accommodating pivotal movements crucial for various tasks.

c. The wrist:

The wrist is situated at the distal end of the upper limb and acts as a bridge between the forearm and hand, facilitating optimal positioning for grasping and manipulation. The

wrist complex has two degrees of freedom, allowing for ulnar/radial deviation and flexion/extension movements, which are essential for precise hand positioning and dexterity for intricate tasks.

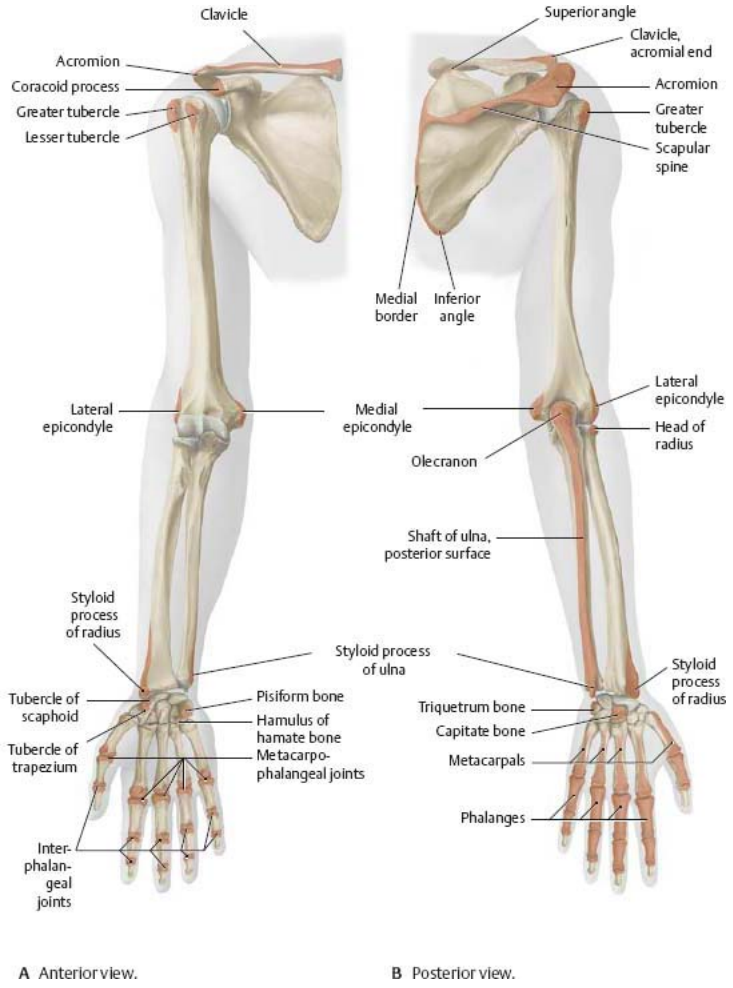

Figure 2.1: Biomechanics of upper limb [74].

2.2.2 Biomechanics of upper limb movement:

The upper limb boasts a remarkable versatility, offering a total of nine DoF in its motion, excluding the intricate joints of the fingers [75]. Let's delve into the specific movements afforded by each major joint:

1. Shoulder joint:

Often considered analogous to a ball joint, the shoulder joint permits a broad spectrum of movement through three principal rotations. These include:

-Flexion / Extension (Figure 2.2.g): Forward and backward movements of the arm.

- Abduction / Adduction (Figure 2.2.h): Outward and inward movements away from and toward the body's midline.

- Internal Rotation / External Rotation (Figure 2.2.i): Rotational movements inwards and outwards.

In addition, the sternoclavicular joint contributes two degrees of freedom:
- Elevation/depression: The elevation and depression of the shoulder joint.
- Retraction/protraction: The shoulder ball joint undergoes a shift in its center of rotation as it moves backward and forward.

Together, these movements provide the shoulder with a total of five degrees of freedom [76].

1. Elbow joint:

The elbow, which is characterized by its hinge-like structure, facilitates two principal movements:
- Flexion / extension (Figure 2.2.d): Bending and straightening of the forearm.
- Pronation / supination (Figure 2.2.f): Are rotational movements of the forearm that allow the palm to face downward (pronation) or upward (supination).

1. Wrist joint:

The wrist is a distal joint that offers two pivotal degrees of freedom.
- Flexion / extension (Figure 2.2.a): Upward and downward movements of the hand.
- Ulnar deviation / radial deviation (Figure 2.2.b): The hand should be moved in a side-to-side fashion, with the ulna (little finger side) or radius (thumb side) being tilted in the direction of the movement [77].

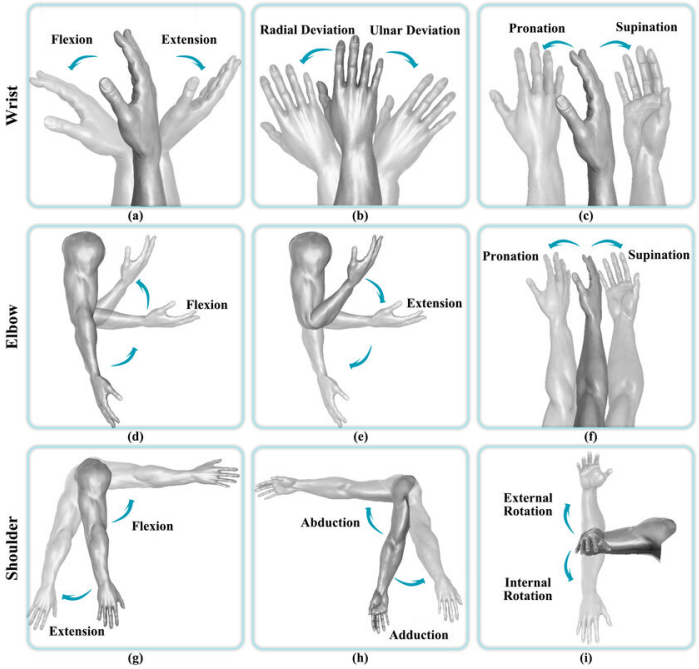

Figure 2.2: Upper limb movements [78]

2.2.3 Mechanical structure of ULEL:

ULEL features three active revolute joints, enabling flexion/extension movements at the shoulder, elbow, and wrist joints. Additionally, it is connected to a frame base via a passive

ball joint, with the capability to block or release the ball via an adjustable friction system. Figure 2 illustrates the mechanical architecture of ULEL.

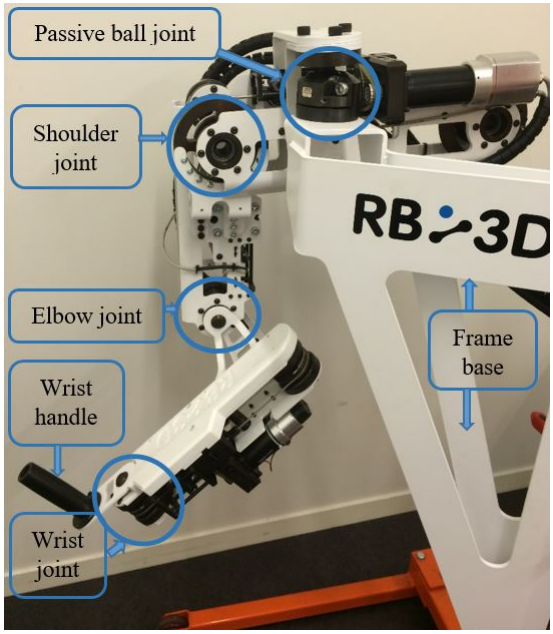

Figure 2.3: Mechanical design of ULEL.

It is evident that ULEL is comprised of four modules. The frame module, which serves as the base, is equipped with a height-adjustable stand that employs a hydraulic system, thus ensuring that the shoulder axis of the exoskeleton aligns with that of the subject. The frame module's carrier is designed with wheels that can be maneuvered with ease, with one of them equipped with a brake. This innovative system enables the exoskeleton to be operated without the subject lifting it. The shoulder module incorporates a revolute joint with an onboard actuator, which is connected to the frame through a passive adjustable ball joint. The arm module is situated on the shoulder and contains the actuator that is responsible for elbow movement. Furthermore, the wrist movement is driven by the onboard actuator within the forearm module. The ULEL actuation and transmission system is based on an embedded screw and cable mechanism [79]. Each joint is equipped with a direct current (DC) brushless motor and an encoder to measure the angle of rotation. ULEL is designed to interact directly with the user, which necessitates the inclusion of safety features. Consequently, a power-off applied brake and limit switches are incorporated into each active joint. Table 2.1 provides a summary of the specifications for the three ULEL active axes.

Table 2.1: *Mechanical properties of ULEL.*

Joints	Shoulder	Elbow	Wrist
Motors	DC brushes		
Movement	Flexion / Extension		
Transmission	Screw and Cable System (SCS)		
Magnitude (deg)	90	120	80
Transmission ratio	251.3	167.6	47.1
Velocity (rpm)	18.39	41.93	149
Torque (Nm)	85.08	23.9	6.72
Power (W)	200	150	150

The actuation and transmission system of ULEL is based on an embedded screw and cable system (SCS). The joint is driven by a standard push-pull cable, while the cable is driven on one side by a ball screw locked in rotation, which translates directly in its nut without any linear guiding Figure 2.4. This system enables high operational torques thanks to high reduction ratios. Moreover, it permits high reversibility and back drivability. The alignment of the motor shaft with the cable provides a compact structure with a low inertia.

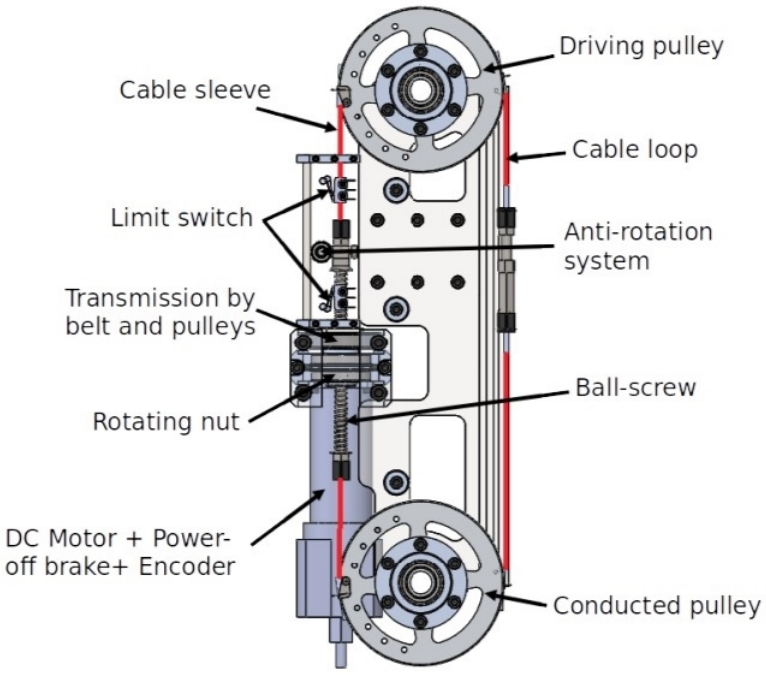

Figure 2.4: *Embedded shoulder actuator.*

2.3 ULEL exoskeleton modeling:

Modeling plays a pivotal role in the characterization of the utilized device and in the design process of prospective controllers. Models are employed to conduct simulations, which

facilitate the testing of system behavior and validation of the control schemes in a safe manner. Additionally, they are utilized to identify the kinematic and dynamic parameters that are essential for control and simulations.

The modeling of ULEL exoskeleton is carried out using the modified Denavit Hartenberg (DH) method [80]. The kinematic diagram of the ULEL exoskeleton is illustrated in 2.5, where $R_i(O_i, x_i, y_i, z_i)$ represents the frame attached to the link i and q_i is the joint angle such that: $q = [q_1\, q_2\, q_3]^T$, and the range of motion is detailed in Table 2.2.

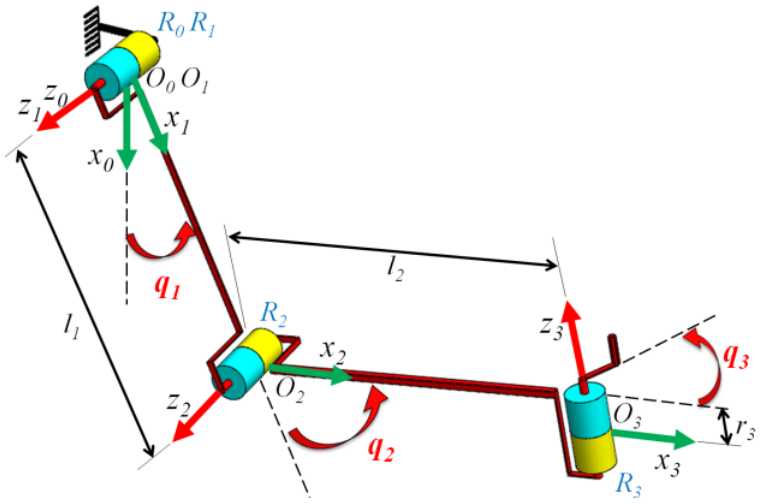

Figure 2.5: Kinematic diagram of ULEL [58].

Table 2.2: *Field of motion of ULEL [58].*

Joint	Movement	Range (deg)
Shoulder	Flexion / Extension	$0 \rightarrow 90$
Elbow	Flexion / Extension	$10 \rightarrow 110$
Wrist	Flexion / Extension	$-40 \rightarrow +40$

2.3.1 Geometric model:

This study focuses on geometrically modeling a 3 DoF exoskeleton robot, laying the groundwork for subsequent mechanical and kinematic analyses. The exoskeleton comprises of an interconnected links and joints, where each is defined by a specific geometric parameters and constraints. By utilizing the Direct Geometric Model (DGM), we can accurately determine the position and orientation of the end-effector, such as the wrist handle, based on the joint configurations.

The general transformation matrix can be given as:

$$ {}^{i-1}T_i = \begin{bmatrix} \cos(\theta_i) & -\sin(\theta_i) & 0 & d_i \\ \cos(\alpha_i)\sin(\theta_i) & \cos(\alpha_i)\cos(\theta_i) & -\sin(\alpha_i) & -r_i\sin(\alpha_i) \\ \sin(\alpha_i)\sin(\theta_i) & \sin(\alpha_i)\cos(\theta_i) & \cos(\alpha_i) & r_i\cos(\alpha_i) \\ 0 & 0 & 0 & 1 \end{bmatrix} \tag{2.1} $$

Where:

- α_i is the angle between $z_{i-1}$and z_i around x_{i-1}.
- d_i is the distance between $z_{i-1}$and z_i along x_{i-1}.
- θ_i is the angle between $x_{i-1}$and x_i around z_i.
- r_i is the distance between $x_{i-1}$and x_i along z_i.

Through the analyses of the kinematic diagram depicted in Figure 2.5, we can obtain the DH parameters as follows:

Table 2.3: *Modified DH parameters.*

i	α_i	d_i	θ_i	r_i
1	0	0	q_1	0
2	0	l_1	q_2	0
3	$-\frac{\pi}{2}$	l_2	q_3	r_3

By using the transformation matrix 2.1 and Table 2.3, we can deduce:

$$ {}^{0}T_1 = \begin{bmatrix} C_1 & -S_1 & 0 & 0 \\ S_1 & C_1 & 0 & 0 \\ 0 & 0 & 1 & 0 \\ 0 & 0 & 0 & 1 \end{bmatrix} $$

$$ {}^{1}T_2 = \begin{bmatrix} C_2 & -S_2 & 0 & l_1 \\ S_2 & C_2 & 0 & 0 \\ 0 & 0 & 1 & 0 \\ 0 & 0 & 0 & 1 \end{bmatrix} $$

$$ {}^{2}T_3 = \begin{bmatrix} C_3 & -S_3 & 0 & l_2 \\ 0 & 0 & 1 & r_3 \\ -S_3 & -C_3 & 0 & 0 \\ 0 & 0 & 0 & 1 \end{bmatrix} $$

Where:

C_i *and* S_i are $\cos(q_i)$ and $\sin(q_i)$, respectively.

The resultant transformation matrix is obtained by multiplying the above calculated matrices.

$$ {}^{0}T_3 = \begin{bmatrix} C_{12}C_3 & -C_{12}S_3 & -S_{12} & l_1C_1 + l_2C_{12} - r_3S_{12} \\ S_{12}C_3 & -S_{12}S3 & C_{12} & l_1S_1 + l_2S_{12} + r_3C_{12} \\ -S_3 & -C_3 & 0 & 0 \\ 0 & 0 & 0 & 1 \end{bmatrix} \tag{2.2} $$

Where:
C_{ij} *and* S_{ij} are $\cos(q_i + q_j)$ and $\sin(q_i + q_j)$, respectively.

In robotics, it is widely recognized [80] that given an arbitrary point A located at the Cartesian coordinates $({}^iA_x, {}^iA_y, {}^iA_z)$ relative to frame R_i,the Cartesian coordinates $({}^jA_x, {}^jA_y, {}^jA_z)$ of A relative to another frame R_j can be computed as follows:

$$ {}^jA = {}^jT_i \times {}^iA \tag{2.3}$$

Where:
${}^iA = \begin{bmatrix} {}^iA_x & {}^iA_y & {}^iA_z & 1 \end{bmatrix}^T$, ${}^jA = \begin{bmatrix} {}^jA_x & {}^jA_y & {}^jA_z & 1 \end{bmatrix}^T$are the homogeneous coordinates of point A with respect to R_i and R_j, respectively.

Let the Cartesian coordinates of the end-effector (terminal fixed point) of ULEL be presented in R_3 frame by $({}^3A_x, {}^3A_y, {}^3A_z)$. The absolute Cartesian coordinates of this position in the frame R_0can be given by:

$$\begin{bmatrix} {}^0A_x \\ {}^0A_y \\ {}^0A_z \\ 1 \end{bmatrix} = {}^0T_3 \begin{bmatrix} {}^3A_x \\ {}^3A_y \\ {}^3A_z \\ 1 \end{bmatrix} \tag{2.4}$$

Substituting 2.2 in 2.4 yields the DGM of ULEL exoskeleton as follows:

$$\begin{cases} {}^0A_x = {}^3A_xC_{12}C_3 - {}^3A_yC_{12}S_3 - {}^3A_zS_{12} + l_1C_1 + l_2C_{12} - r_3S_{12} \\ {}^0A_y = {}^3A_xS_{12}C_3 - {}^3A_yS_{12}S3 - {}^3A_zC_{12} + l_1S_1 + l_2S_{12} + r_3C_{12} \\ {}^0A_z = -{}^3A_xS_3 - {}^3A_yC_3 \end{cases} \tag{2.5}$$

2.3.2 Kinematic model:

The Direct Kinematic Model (DKM) establishes the relationship between the joint velocities and the end-effector velocity. This relationship can be expressed as $\dot{\chi} = J(q)\dot{q}$, where $\dot{\chi}$ denotes the velocity of the end-effector, $\dot{q} \in \mathbb{R}^3$ represents the vector of joint velocities, and $J(q) \in \mathbb{R}^{3\times3}$ is the Jacobian matrix. The Jacobian matrix, which is a function of the joint parameters q, provides a linear approximation of this relationship by mapping the joint velocities to the corresponding end-effoctor velocities. Each element of the Jacobian matrix is derived from the partial derivatives o the end-effector's position with respect o each joint variable, capturing how changes in join angles affect the robot's terminal motion.

$$J_{i,j} = \frac{\partial X_i}{\partial q_j} \tag{2.6}$$

where $J_{i,j}$ represents the element (i, j) of the Jacobian matrix J.

Let χ be the position of the robot's terminal and defined by:

$$\chi = \begin{bmatrix} {}^0A_x \\ {}^0A_y \\ {}^0A_z \\ 1 \end{bmatrix}$$

Applying Equation 2.6 to the DGM results the following Jacobian matrix J_v of the end-effector for the linear velocity:

$$
{}^{0}J_v = \begin{cases}
J_{1,1} = -{}^{3}A_x S_{12} C_3 + {}^{3}A_y S_{12} S_3 - {}^{3}A_z C_{12} - l_1 S_1 - l_2 S_{12} - r_3 C_{12} \\
J_{1,2} = -{}^{3}A_x S_{12} C_3 + {}^{3}A_y S_{12} S_3 - {}^{3}A_z C_{12} - l_2 S_{12} - r_3 C_{12} \\
J_{1,3} = -{}^{3}A_x C_{12} S_3 - {}^{3}A_y C_{12} C_3 \\
J_{2,1} = {}^{3}A_x C_{12} C_3 - {}^{3}A_y C_{12} S_3 - {}^{3}A_z S_{12} + l_1 C_1 + l_2 C_{12} - r_3 S_{12} \\
J_{2,2} = {}^{3}A_x C_{12} C_3 - {}^{3}A_y C_{12} S_3 - {}^{3}A_z S_{12} + l_2 C_{12} - r_3 S_{12} \\
J_{2,3} = -{}^{3}A_x S_{12} S_3 - {}^{3}A_y S_{12} C_3 \\
J_{3,1} = 0 \\
J_{3,2} = 0 \\
J_{3,3} = -{}^{3}A_x C_3 + {}^{3}A_y S_3
\end{cases} \tag{2.7}
$$

Based on the ULEL's configuration depicted in Figure 2.5, we can see that the Cartesian coordinate of the point A in the $x-axis$ is equal to zero. Hence, the Equation 2.7 becomes:

$$
{}^{0}J_v = \begin{cases}
J_{1,1} = {}^{3}A_y S_{12} S_3 - {}^{3}A_z C_{12} - l_1 S_1 - l_2 S_{12} - r_3 C_{12} \\
J_{1,2} = {}^{3}A_y S_{12} S_3 - {}^{3}A_z C_{12} - l_2 S_{12} - r_3 C_{12} \\
J_{1,3} = -{}^{3}A_y C_{12} C_3 \\
J_{2,1} = -{}^{3}A_y C_{12} S_3 - {}^{3}A_z S_{12} + l_1 C_1 + l_2 C_{12} - r_3 S_{12} \\
J_{2,2} = -{}^{3}A_y C_{12} S_3 - {}^{3}A_z S_{12} + l_2 C_{12} - r_3 S_{12} \\
J_{2,3} = -{}^{3}A_y S_{12} C_3 \\
J_{3,1} = 0 \\
J_{3,2} = 0 \\
J_{3,3} = {}^{3}A_y S_3
\end{cases} \tag{2.8}
$$

In addition, The linear ${}^{i}v_i \in \mathbb{R}^3$ and angular ${}^{i}\omega_i \in \mathbb{R}^3$ velocities of the system can be expressed in relative to the last frame R_n $(n = 3)$ using the Jacobian matrices as follows:

Linear velocity:

$$
{}^{n}v_n = {}^{n} J_v(q)\dot{q} \tag{2.9}
$$

Angular velocity:

$$
{}^{n}\omega_n = {}^{n} J_\omega(q)\dot{q} \tag{2.10}
$$

where J_v,J_w $\in \mathbb{R}^{3\times3}$ are the Jacobian matrices of the linear and angular velocities, respectively.

More details about the calculation of the linear and angular velocities, in addition, the Jacobian matrices is explained in the next subsection.

2.3.3 Dynamic model:

For systems involving multiple rigid bodies, various dynamic modeling methods are available. The Euler–Lagrange method stands out as a well-established and classical approach for dynamic modeling of multi-rigid-body systems . This method involves differentiating

the system variables and time based on energy terms. While it might seem more complex than Newtonian mechanics for simpler systems, the Euler–Lagrange method becomes more manageable as the system's complexity increases [81]. It relies on two fundamental Equations: one for linear motion (translational) and the other for rotational motion. To begin, we define the Lagrangian functions as follows:

$$L = T - U \tag{2.11}$$

Where T & U denotes the kinetic and the potential energy of the system, respectively.

and the system's output torques can be written as:

$$\tau_i = \frac{d}{dt}\frac{\partial L}{\partial \dot{q}_i} - \frac{\partial L}{\partial q_i} \tag{2.12}$$

where $q_i, \dot{q}_i \in \mathbb{R}^3$ are the system's joint i position and velocity vectors, respectively. and $\tau_i \in \mathbb{R}^n$ is the exoskeleton torque or joint i.

Kinetic energy T

The generalized formula of the kinetic energy of the exoskeleton system is given by:

$$T = \frac{1}{2}\dot{q}^T M(q)\dot{q} \tag{2.13}$$

Where $M(q) \in \mathbb{R}^{3\times3}$ represents the robot's non-singular inertia matrix, which is symmetric and positive definite.

The Equation 2.13 can also be presented in König form as follows:

$$T = \frac{1}{2}\sum_{i=1}^{3}\left(m_i {}^i v_i^{Ti} v_i + m_i {}^i r_{ci}^T S({}^i v_i) {}^i\omega_i + {}^i\omega_i^{Ti} I_i {}^i\omega_i\right) \tag{2.14}$$

with:

$${}^{i+1}v_{i+1} = {}^{i+1}R_i({}^i v_i + {}^i\omega_i \wedge {}^i P_{i+1}) \tag{2.15}$$

and

$${}^{i+1}\omega_{i+1} = {}^{i+1}R_i {}^i\omega_i + \dot{q}_{i+1} {}^{i+1}Z_{i+1} \tag{2.16}$$

and

$$I_i = \begin{pmatrix} I_{i,xx} & I_{i,xy} & I_{i,xz} \\ & I_{i,yy} & I_{i,yz} \\ symm & & I_{i,zz} \end{pmatrix}$$

Where:

- ${}^i P_{i+1} \in \mathbb{R}^3$ is the distance between the frame $i+1$ to i.
- ${}^{i+1}Z_{i+1} \in \mathbb{R}^3$ is the unit vector of the same frame along $z_i - axis$ which equals to $[0\ \ 0\ \ 1]^T$.

- $m_i \in \mathbb{R}$ is the mass of the link i.
- ${}^{i}v_i \in \mathbb{R}^3$ is the linear velocity vector of the same frame relative to center of mass.
- ${}^{i}\omega_i \in \mathbb{R}^3$ is the angular velocity vector of the same frame relative to center of mass.
- ${}^{i}r_{ci} = [{}^{i}x_{mi} \ {}^{i}y_{mi} \ {}^{i}z_{mi}]^T \in \mathbb{R}^3$ is the center of mass coordinates of link i of the same frame.
- $S(.)$ Is the skew-symmetric matrix operator.
- ${}^{i}I_i \in \mathbb{R}^{3\times3}$ is the inertia matrix of the same frame around the center of mass.

Potential energy U

The potential energy of the system is given by:

$$U = \sum_{i=1}^{3} U_i \tag{2.17}$$

with:

$$U_i = -m_i g^T r_{0,ci} = -m_i g^T ({}^{i}P_{i+1} + {}^{i} r_{ci})$$

$$U = \sum_{i=1}^{3} -m_i g^T ({}^{i}P_{i+1} + {}^{i} r_{ci}) \tag{2.18}$$

where: $g \in \mathbb{R}^3$ is the gravity acceleration vector.

Friction D

For modeling friction, a wide range of models have been proposed in the literature [80, 82–84]. The combination of viscous and Coulomb frictions for the robot joints can be expressed in following model:

$$D_i(\dot{q}) = -F_{v,i}\dot{q}_i - F_{c,i}sign(\dot{q}_i) \tag{2.19}$$

Where $F_{v,i}(\dot{q}) = diag(F_{v,1}, F_{v,2}, F_{v,3}) \in \mathbb{R}^{3\times3}$ is a diagonal matrix that represents the viscous friction; and $F_{c,i}(\dot{q}) = diag(F_{c,1}, F_{c,2}, F_{c,3}) \in \mathbb{R}^{3\times3}$ is a also a diagonal matrix which depicts the Coulomb friction.

We have now established the dynamics of the exoskeleton. The inverse dynamic model of the system can be written as:

$$M(q)\ddot{q} + C(q,\dot{q})\dot{q} + G(q) = \tau + D(\dot{q}) \tag{2.20}$$

where: $M(q) \in \mathbb{R}^{3\times3}$ is the non-singular inertia matrix; $C(q,\dot{q}) \in \mathbb{R}^{3\times3}$ is the Coriolis and centrifugal matrix; $G(q) \in \mathbb{R}^3$ represent the gravity forces vector; $D(\dot{q}) \in \mathbb{R}^3$ is the dissipation term vector; $\tau_{exo} \in \mathbb{R}^3$ is the exoskeleton's torques.

The matrices and vectors presented below are derived from the calculated terms of the dynamic model 2.20, which are obtained by applying the following Equations:2.14, 2.18, and 2.19, then substituting them into Equation 2.12.

- Trigonometric transformation:
The simplification of the next Equations is based on the following Equations.

$$\begin{cases} S1 = \sin(q_1) \\ C1 = \cos(q_1) \\ S12 = \sin(q_1 + q_2) \\ C12 = \cos(q_1 + q_2) \end{cases}$$

- Inertia matrix M:

$$\begin{aligned}
M_{11} = {} & 2.l_1.m_2.(x_{m_2}.C1 + y_{m_2}S1).C12 - 2.l_1.m_2.(y_{m_2}.C1 - x_{m_2}.S1).S12 + \\
& (l_1^2 + x_{m_2}^2 + y_{m_2}^2).m_2 + m_1.(x_{m_1}^2 + y_{m_1}^2) + I_1 + I_2 \\
M_{12} = {} & l_1.m_2.(x_{m_2}.C1 + y_{m_2}S1).C12 + l_1.m_2.(x_{m_2}.S1 - y_{m_2}.C1).S12 + m_2.(x_{m_2}^2 + y_{m_2}^2) + I_2 \\
M_{13} = {} & 0 \\
M_{21} = {} & M_{12} \\
M_{22} = {} & I_2 + m_2.(x_{m_2}^2 + y_{m_2}^2) \\
M_{23} = {} & 0 \\
M_{31} = {} & M_{13} \\
M_{32} = {} & M_{23} \\
M_{33} = {} & I_3
\end{aligned}$$

- Coriolis and centrifugal matrix C:

$$\begin{aligned}
C_{11} = {} & l_1\,\dot{q_2}\,((x_{m_2}S1 - y_{m_2}C1)\,C12 - S12\,(x_{m_2}C1 + y_{m_2}S1))\,m_2 \\
C_{12} = {} & (-l_1\,m_2\,(x_{m_2}C1 + y_{m_2}S1)\,S12 - l_1\,m_2\,(y_{m_2}\,C1 + x_{m_2}S1)\,C12)\,\dot{q_1} + \\
& (-l_1\,m_2\,(x_{m_2}C1 + y_{m_2}S1)\,S12 + l_1\,m_2\,(x_{m_2}\,S1 - y_{m_2}C1)\,C12)\,\dot{q_2} \\
C_{13} = {} & 0 \\
C_{21} = {} & (2\,l_1\,m_2\,(y_{m_2}C1 - x_{m_2}S1)\,C12 + l_1\,m_2\,(x_{m_2}\,S1 - y_{m_2}C1)\,C12 + \\
& l_1\,m_2\,(x_{m_2}C1 + y_{m_2}S1)\,S12\,\dot{q_1}) \\
C_{22} = {} & 0 \\
C_{23} = {} & 0 \\
C_{31} = {} & 0 \\
C_{32} = {} & 0 \\
C_{33} = {} & 0
\end{aligned}$$

- Gravity vector G:

$$\begin{aligned}
G_1 = {} & m_1.g.(x_{m_1}.S1 + y_{m_1}.C1) + m_2.g.(x_{m_2}.S12 + y_{m_2}.C12 + l_1.S1) \\
G_2 = {} & m_2.g.(x_{m_2}.S12 + y_{m_2}.C12) \\
G_3 = {} & 0
\end{aligned}$$

where $g = 9.81\,m/s^2$

- Dissipation vector D:

$$\begin{aligned}
D_1 = {} & F_{v_1}.\dot{q_1} + F_{c_1}.sign(\dot{q_1}) \\
D_2 = {} & F_{v_2}.\dot{q_2} + F_{c_2}.sign(\dot{q_2}) \\
D_3 = {} & F_{v_3}.\dot{q_3} + F_{c_3}.sign(\dot{q_3})
\end{aligned}$$

Remarque: The zeros showed in the inertia and Coriolis matrices are due to the fact that the last articulation is considered as a rigid mass.

2.4 Conclusion:

This chapter presents a comprehensive exploration of the domain of exoskeleton modeling, with particular attention paid to the ULEL exoskeleton. A comprehensive analysis of pivotal areas, including geometric, kinematic, and dynamic aspects, was conducted with the objective of elucidating the theoretical foundations and practical implications associated with exoskeleton modeling. Finally, a detailed dynamic model of the ULEL exoskeleton robot was established. The following chapter will provide a detailed discussion of the PSO algorithm, outlining its applications and relevance to the control strategies discussed in this chapter.

Chapter 3

Particle Swarm Optimization (PSO)

3.1 Introduction:

Particle Swarm Optimization represents a highly effective population-based optimization algorithm, drawing inspiration from the collective behavior observed in nature, particularly the social dynamics of bird flocks and fish schools. PSO was developed as a result of research efforts to emulate the collective intelligence observed in natural systems. It has since become a widely utilized technique for solving optimization problems across various domains.

The history and development of PSO can be traced back to the early 1990s, with Dr. James Kennedy and Dr. Russell Eberhart being primarily credited for their seminal work published in 1995 [85]. This introduced PSO as an optimization algorithm based on the principles of social interaction and cooperation. Since then, PSO has undergone continuous refinement and adaptation by researchers worldwide, leading to numerous variants and applications across diverse fields.

The essence of PSO is a straightforward yet sophisticated concept: a population of potential solutions, known as particles, navigates the solution space to identify optimal solutions. Each particle represents a potential solution and modifies its position in accordance with its own experiences and the collective knowledge of the swarm.

The fundamental principles underlying the PSO algorithm are as follows:

- *Particles* which represent individuals within the swarm, each associated with a position and velocity in the solution space.

- *The fitness function* is defined as the objective to be optimized, thereby guiding the search for optimal solutions.

- *Velocity and Position Updates:* The velocity and position of particles in the PSO undergo updates influenced by two main factors. Firstly, each particle's velocity and position are adjusted based on its own optimal solution, referred to as pbest, which signifies the velocity and position that would result in the best individual experience. Secondly, the global best-known solution, or gbest, exerts an influence on these adjustments. In contrast to pbest, which is specific to each particle, gbest represents the optimal velocity and position for the entire swarm. This adjustment mechanism, shaped by cognitive and social influences, aims to achieve a balance between exploration and exploitation within the solution space, which is defined as the range of all potential outcomes within given constraints.

This chapter introduces the Particle Swarm Algorithm and its applications. It starts by explaining PSO's basics, followed by a detailed look at how the algorithm works. Different versions and adaptations of PSO are then discussed. Afterward, the chapter explores where PSO is used in real-world scenarios and how its parameters are fine-tuned for optimal performance. It also touches upon the challenges faced and potential future directions for PSO.

3.2 Algorithm description:

The following detailed description presents a comprehensive overview of the PSO algorithm, accompanied by a clear exposition of the role of parameters and pseudocode, which explains the algorithm's operational mechanics.

3.2.1 PSO algorithm:

A- Initialization phase:

- Initialize the swarm of particles randomly within the solution space.
- Assign initial velocities to the particles in a random manner.

B- Velocity and position updates:

- For each particle in the swarm –> Update the particle's velocity using the following formula:

$$V_i^{j+1} = w^j V_i^j + c_1 \left(P_i^j - X_i^j\right) + c_2 \left(G^j - X_i^j\right) \tag{3.1}$$

where j the iteration and

- $c_1,\ c_2 \in \mathbb{R}$ are positive constants.
- $P_i^j \in \mathbb{R}^m$ is the personal best vector of the i-th particle at the iteration j.
- $G^j \in \mathbb{R}^m$ is the global best vector of all particles at the iteration j.
- $X_i^j,\ X_i^{j+1} \in \mathbb{R}^m$ are the current and updated position vectors separately of the i-th particle.
- $V_i^j,\ V_i^{j+1} \in \mathbb{R}^m$ are the current and updated velocity vectors, respectively of the i-th particle.
- $w^j \in \mathbb{R}$ is a constant positive weigh.

- Update the particle's position using the following Equation:

$$X_i^{j+1} = X_i^j + V_i^{j+1} \tag{3.2}$$

C- Fitness evaluation: The fitness of each particle must be evaluated using a cost function that measures the quality of the solution represented by the particle's position.

D- Termination conditions: The algorithm should be terminated if a predefined stopping criterion is met. This criterion could be, for example, reaching a maximum number of iterations, achieving a satisfactory solution, or stagnation of the algorithm.

3.2.2 Significance of parameters in PSO algorithm:

- Swarm Size: This parameter is constant and determines the number of particles present in the swarm, which influences the swarm's exploration and exploitation abilities.

- Inertia Weight (w): This concept balances the trade-off between exploration and exploitation. High inertia values encourage exploration, while low values promote exploitation.

- Acceleration Coefficients (C_1 and C_2): They are essential to ascertain the influence of personal best positions (P) and global best positions (G) on particle velocity updates.

- Termination Criteria: It is necessary to determine the point at which the algorithm should be terminated in order to prevent the unnecessary expenditure of computational resources and to ensure convergence.

3.2.3 Pseudocode:

The below descripted code represents the standard PSO version.

1. Initialize swarm of particles randomly
2. Initialize personal best position ($Pbest$) for each particle
3. Initialize global best position ($Gbest$) of the swarm
4. Set maximum number of iteration or convergence criteria
5. Loop {Iteration = Max}
   {
   a. For each particle in the swarm:
      Update particle velocity using formula 3.1
      Update particle position using formula 3.2
      Evaluate fitness of particle
      Update personal best position if fitness improves
      Update global best position if fitness improves
   b. Incerement iteration counter
   } End loop

3.3 Variant and modifications:

Particle Swarm Optimization has attracted considerable interest in the field of optimization due to its simplicity, effectiveness, and versatility. Over time, researchers have proposed a number of variations and modifications to the basic PSO algorithm, with the aim of enhancing its performance, addressing the local optimal stacking issue, and extending its applicability to a range of diverse optimization problems. This section examines several prominent variants and modifications of PSO, including swarm initialization, mutation operators' updating, the constriction coefficient approach, inertia weight updating [86], and Hybrid PSO algorithms.

3.3.1 Initialization:

The initialization of particles in PSO is crucial for its performance. Poor initialization can lead to inefficient exploration of the solution space, resulting in difficulty finding the optimal solution. The success of PSO heavily relies on well-designed initialization strategies, which guide the algorithm toward promising regions and accelerate convergence. Therefore, careful attention to initialization is essential for achieving robust and efficient optimization outcomes [87–91].

3.3.2 Mutation operators:

To improve the performance of PSO and to avoid local minima stagnation, researchers have developed several variants that incorporate mutation operators. These mutations target either the global or local best particle, introducing diversity into the search process.

Applying various techniques encourages exploration of new regions in the solution space, enabling more effective navigation of complex landscapes and avoiding premature convergence [89, 92–98].

3.3.3 Constriction coefficient approach:

The constriction coefficient approach is a modification of the standard PSO algorithm aimed at improving its convergence behavior and stability. In tradition, PSO's particles update their velocities based on three main components: inertia, cognitive (personal best), and social (global best) terms. However, these updates can sometimes lead to excessive particle velocities leading to overshooting and instability, especially in high-dimensional or complex optimization problems.

The constriction coefficient approach incorporates a constriction factor, denoted χ, into the velocity update Equation to regulate particle motion. By adjusting the particle velocity according to the constriction factor, this approach optimizes the convergence properties and reduces the risk of divergence, thereby increasing the effectiveness of the PSO algorithm. By introducing an additional parameter to control particle velocity updates, the approach ensures that particle movements are constrained, preventing them from growing indefinitely and improving the overall stability of the optimization process. The use of the constraint factor provides a balanced trade-off between exploration and exploitation, leading to more efficient and reliable optimization results [99–101].

3.3.4 Inertia weight:

The inertia weight plays a key role in balancing the exploration-exploitation tradeoff in the PSO algorithm, similar to the constriction coefficient. A higher inertia weight value promotes exploration by encouraging particles to explore a larger search space. Conversely, a lower inertia weight value emphasizes exploitation, allowing particles to focus on the refinement of promising solutions. Several strategies for manipulating the inertia weight have been explored by researchers. Some use a fixed inertia weight, while others use linearly or nonlinearly decreasing schemes [92, 102–107].

3.3.5 Hybrid PSO algorithms:

Hybrid PSO algorithms integrate PSO with other optimization techniques or problem-solving approaches in order to leverage the strengths of each method and overcome their respective limitations. In the literature, the local optimum problem in PSO has been discussed, and various variants of PSO algorithms have been developed to address this problem. For example, researchers have attempted to incorporate evolutionary operators such as crossover, mutation, selection, and the Differential Evolution (DE) algorithm itself into PSO. As a result, hybrid versions of PSO have been tested and produced, including hybrid evolutionary PSO [108], genetic algorithm (GA) and PSO [109, 110], genetic programming-based adaptive evolutionary hybrid PSO [Psogp: a genetic programming based adaptive evolutionary hybrid particle swarm optimization], and many others [111]. Such improvements perform well with PSO and have the potential to avoid getting stuck at the local optimum. However, the problem of premature convergence still exists in

some high-dimensional complex problems, even when the local optima obstacle is absent. Therefore, PSO does not always work properly for high-dimensional models [112].

There are unique advantages, limitations, and applications to each variant and modification of PSO. The constriction coefficient approach improves convergence properties through balancing between exploration and exploitation. Hybrid PSO algorithms provide flexibility and adaptability to different optimizing scenarios. In addition to these variations, several key factors have a significant impact on the performance and effectiveness of PSO: Initialization sets the initial positions and velocities of the particles, which affects the convergence behavior; mutation operators introduce diversity into the search process, which mitigates stagnation at local minima; and the inertia weight parameter balances exploration and exploitation. Tuning these factors along with PSO variants provides a comprehensive understanding of the algorithm's capabilities, limitations, and potential applications in various optimization tasks.

More details about variants and improvements of the PSO are depicted in Figure 3.1.

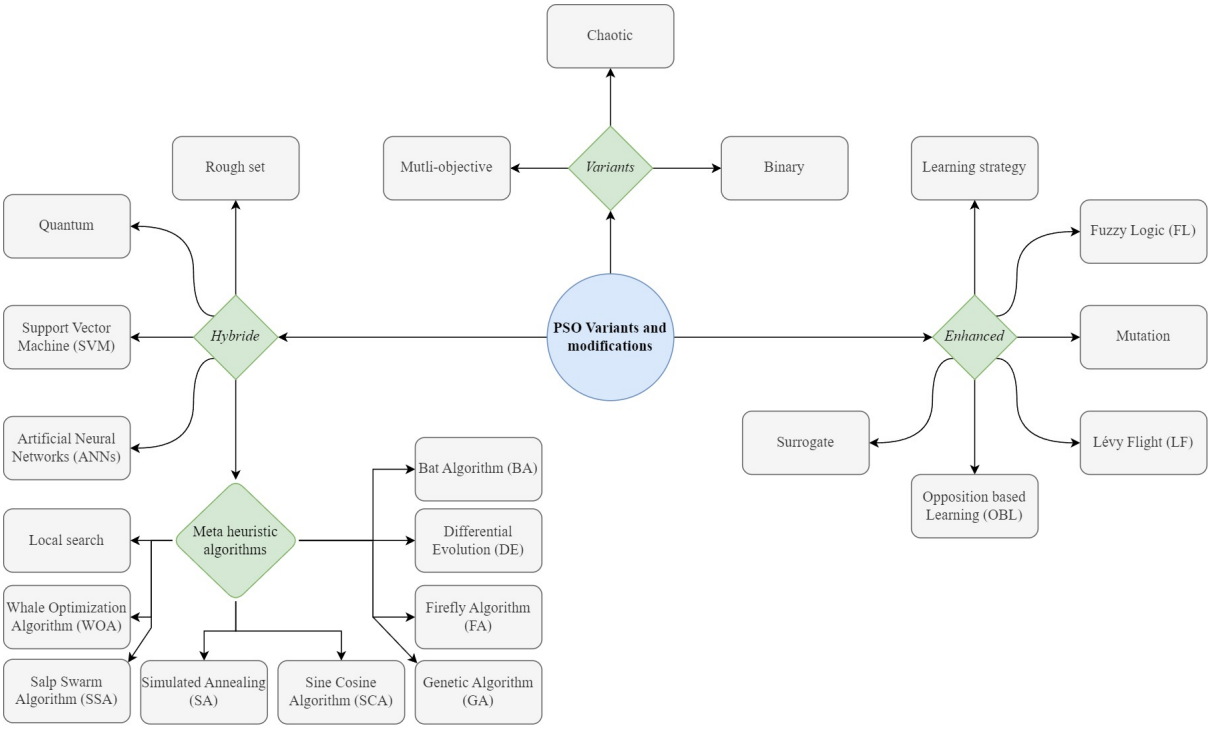

Figure 3.1: PSO methods classification.

3.4 Application of PSO:

The PSO algorithm has been demonstrated to be effective and adaptable in addressing a diverse range of optimization challenges across various domains. This section provides a comprehensive categorization of the practical applications of PSO in different real-world fields [112], including health care, environmental, industrial, commercial, smart city, and general aspects. A summary of PSO applications is illustrated in Figure 3.2.

3.4.1 Health care:

PSO can be used in healthcare for tasks such as optimizing treatment plans, measuring drug dosages, diagnosing diseases, and segmentation and classifying of medical images. For example, a disease diagnostic system is presented in [113] for identifying and classifying the most beneficial genes and for Alzheimer's disease diagnosis in [114]. Next, a cancer diagnosis and classification using DNA microarray technology is introduced in [115]. Furthermore, a medical image segmentation, an electrocardiogram (ECG) signal analysis, and an intelligent Leukaemia diagnosis are demonstrated in [116–118], respectively.

3.4.2 Environmental:

PSO can facilitate environmental management by optimizing processes such as waste management, pollution control, and renewable energy generation. For instance, a short-term temperature prediction system utilizing ambient sensors is presented in [119]. Next, a multipurpose water reservoir operation system is introduced in [120]. Then, an atmospheric pollutant concentration forecasting, daily suspended sediment load predicting, and images segmentation and classification of a plants based on leaf pictures systems are presented in [121–123], respectively. Additionally, more applications related to environments are exhibited in [124–127].

3.4.3 Industrial:

In industrial settings, PSO can be utilized to optimize various aspects of manufacturing processes, allocating daily electrical loads, defects prediction, and power dispatch. PSO algorithms can be employed to optimize parameters in manufacturing processes such as the parameters of plastic injection machines, thereby enhancing efficiency, reducing waste, and improving product quality. For example, a logistics planning for food grain industry considering wastages system is developed in [128]. Also, a photovoltaic/thermal system-based building energy performance prediction system has been developed in [129]. Furthermore, an optimal design of a mechatronic quadrotor, nuclear power plant potential faults recognizing and diagnosing, multi-objective optimization design of the airborne electro-optical platform, sizing of an off-grid house with solar panels and wind turbines systems are presented in [125, 130–132], respectively. Moreover, additional applications for industrial purposes are illustrated in [133–135].

3.4.4 Commercial:

PSO is applicable in a multitude of commercial domains, including, but not limited to, marketing, finance, and logistics. To elaborate, it may optimize marketing campaigns by identifying the most effective advertising channels or by optimizing pricing strategies in order to maximize profit. Furthermore, PSO can be employed in the domain of finance for the purpose of cost prediction, profit calculation, and risk assessment. For example, an electric business center location optimization system has been introduced in [136], followed by building materials' prices forecasting system presented in [137]. Next, a profit calculation module is proposed in [138] with a cost prediction of a transmission line project

exhibited in [139]. Finally, a forecasting volatility from financial time series is presented in [140].

3.4.5 Smart city:

In smart cities, PSO can be employed to optimize traffic management by adjusting signal timings and route planning. It can also be utilized to manage energy usage, optimize waste collection routes, aid in urban infrastructure planning, and balance energy supply and demand in smart grids. For instance, managing energy in smart homes system has been proposed in [141]. Next, a forecasting day ahead traffic flow, scheduling shiftable appliances, and building's heating load estimation and controlling systems have been presented in [142–144], respectively. In addition, many applications of PSO in smart city can be found in [145–148].

3.4.6 General aspects:

PSO is applicable to a wide range of domains, including computer science, service allocation, image segmentation, scheduling, prediction, and security management. It optimizes the allocation of resources, enhances the accuracy of image analysis, improves the efficiency of task scheduling, enables the accurate forecasting of outcomes, and strengthens security measures by iteratively refining parameters in order to converge towards optimal solutions. For example, in [149], a permission based detection of android malwares module has been proposed. Next, a job shop scheduling problem, task scheduling in cloud computing, traveling salesman problem, and path planning of multi-robots propositions are presented in [150–154], respectively. Moreover, many applications in various fields are demonstrated in [155–160].

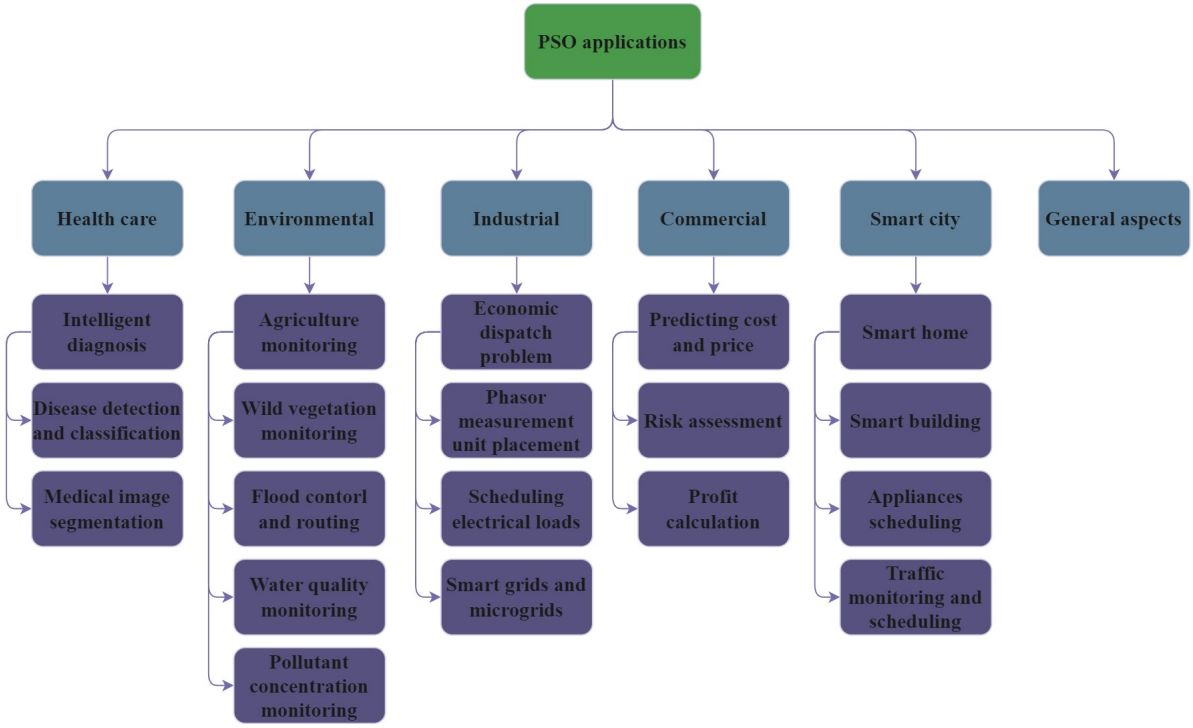

Figure 3.2: PSO applications.

3.5 Challengies and future directions:

Despite its pervasive adoption and efficacy in numerous optimization domains, PSO still necessitates further enhancements. Consequently, this section elucidates the existing limitations of PSO and proposes prospective avenues for its advancement.

3.5.1 Challenges and limitations:

- ***Premature Convergence:*** PSO algorithms may exhibit premature convergence, whereby the swarm reaches suboptimal solutions prematurely, before fully exploring the solution space. This limits the algorithm's ability to identify global optima, particularly in complex, multimodal optimization problems.

- ***Convergence speed controller:*** Despite the typical fast convergence of PSO, there is a possibility that it may be trapped into a local optimum due to premature convergence. Consequently, it is imperative that researchers consider the implementation of a convergence speed controller as a means of achieving the ultimate goal of solving this problem. The convergence speed can be slowed down when the particle prematurely converges. Conversely, when the particle is unable to update its optimal solution in the present moment, the convergence speed is accelerated. For this reason, a significant remaining challenge is the development of an effective convergence speed controller [161].

- ***Scalability issues:*** The scalability of PSO is negatively impacted by an increase in the dimensionality of the search space or when handling a large-scale optimization

problems. The computation complexity of PSO algorithms grows exponentially with the size of the problem, resulting in prolonged computation times and necessity of greater resources. Consequently, a challenge is raised to improve the PSO algorithm, so that it adapts with the high dimensional problems. Indeed, in [162], a high dimensional feature selection problem has been solved by using only a small set of relevant features from a wide range of features.

- ***Memory requirements:*** Storing promising solutions of the PSO can be considered as a performance upgrade. Because the algorithm can reuse historical solutions in subsequent stages to find the optimal solution, as presented in [163].
- ***Parameter and topology selection:*** In PSO, achieving peak performance depends on fine-tuning control parameters, which is often challenging due to a lack of clear guidance. Future research should focus on methods such as simulations, limited-resource parametric analysis, and heuristic-based hyper-parameter selection. Additionally, the effectiveness of PSO in engineering relies heavily on selecting suitable topologies, an area that needs more exploration. Research should consider factors such as topological degree and particle count to identify appropriate deterministic regular topologies [164]. Moreover, the exploration of tree topologies and the suggestion of diverse ones for specific goals, such as optimal PID controller design [165], are vital areas that require further investigation.

3.5.2 Future directions:

In the future, the potential for PSO to contribute to a range of domains is promising, driven by ongoing advancements in optimization techniques and the emergence of new application areas. As computational power continues to increase and interdisciplinary collaboration expands, PSO is poised to play a pivotal role in addressing complex optimization challenges and pushing the boundaries of innovation. In the field of image processing, PSO's capacity to optimize parameters in algorithms for processing colored images presents promising avenues for enhancing image quality, enabling more accurate object detection, and facilitating advanced computer vision applications. In computational biology, PSO serves as a valuable tool for elucidating the intricacies of biological systems. By optimizing parameters in biological models and algorithms, PSO can facilitate protein structure prediction, gene sequence alignment, and the inference of gene regulatory networks. Moreover, in the domain of recommender systems, PSO's capacity to refine recommendation algorithms offers considerable potential for delivering personalized and pertinent content to users across diverse platforms. In summary, as researchers and practitioners continue to investigate new avenues and refine existing methodologies, PSO will continue to evolve and improve across various fields.

3.6 Conclusion:

Particle swarm optimization has emerged as a cornerstone in the realm of optimization, offering a versatile and robust framework for addressing complex optimization problems across diverse domains. This chapter provided a comprehensive understanding of PSO's

significance and potential contributions to the field of optimization through an in-depth exploration encompassing foundational principles, algorithmic descriptions, variants, applications, challenges, and future directions. The synthesis of these key contributions underscores the significance of PSO as a powerful optimization technique with profound implications for research, industry, and societal advancement. As researchers continue to unravel the mysteries of swarm behaviour and optimization dynamics, PSO holds promise for unlocking novel solutions to complex optimization problems, driving innovation, and shaping the future of optimization research and practice. The next chapter will present our principal contribution to the field of robotic rehabilitation and exoskeleton control.

Chapter 4

Real-time adaptive super twisting algorithm based on PSO

4.1 Introduction:

Exoskeleton robots have emerged as a promising tool for enhancing rehabilitation therapy and providing support to therapists. Conventional rehabilitation techniques are characterized by prolonged periods of time, high energy expenditure, and variable outcomes. Given the rising prevalence of stroke, with over 13.7 million new cases annually, conventional approaches are inadequate for effectively treating all patients. Exoskeleton robots present a viable solution for individuals with disabilities, assisting them in regaining limb control [1–5] and being utilized in various domains, including military applications [166, 167].

Despite the advancements in exoskeleton utilization, the industry has yet to widely adopt them for therapeutic purposes. A multitude of research endeavors have been dedicated to the development of control strategies for wearable robots in passive, assistive, and active rehabilitation modes, employing a variety of techniques, including Sliding Mode Control (SMC) [2, 3, 168], neural network control [1, 4, 169–172], adaptive PID control [173–175], EMG-based control [176–180], and impedance control. Among these, the Super Twisting Sliding Mode Control (ST-SMC) stands out due to its robustness and effectiveness in managing nonlinear systems.

This chapter introduces an adaptive ST-SMC algorithm optimized through PSO [181]. The proposed approach addresses the shortcoming of classic ST-SMC, such as offline parameter tuning, by enabling optimal online tuning of controller parameters. This enhancement improves the performance and stability of the control system, making it more effective for real-time applications in exoskeleton robots. Simulation results validate the proposed method, demonstrating its superiority over traditional control techniques.

This chapter begins with an examination of the dynamics of the exoskeleton, which serves as the foundation for our study. We then proceed to present our novel control algorithm that have been developed as part of this thesis. Additionally, we exhibits the simulation and experimental results obtained from the implementation of our new control approach, considering various scenarios to demonstrate its performance and robustness.

4.2 Considered system

The system under examination in this study is comprised of the wearer and the ULEL exoskeleton, designed by RB3D for the LISSI Laboratory. The ULEL features three active revolute joints that enable the flexion and extension movements of the shoulder, elbow, and wrist. Additionally, an adjustable passive ball joint can be used to position the exoskeleton's arm, as illustrated in Figure 4.1. The specifications of the ULEL's three active joints are presented in Table 2.1

4.2.1 Dynamic model

The dynamic model of the examined system that consists of the exoskeleton and the wearer can be expressed by using Euler-Lagrange formalism as follows:

$$M(q)\ddot{q} + H(q, \dot{q}) = \tau_{exo} + \tau_{hum} \tag{4.1}$$

with

$$H(q,\dot{q}) = C(q,\dot{q})\,\dot{q} + G(q) + F(\dot{q})$$

thatand

$$u = \tau_{exo}$$

where $q \in \mathbb{R}^n$, $\dot{q} \in \mathbb{R}^n$ and $\ddot{q} \in \mathbb{R}^n$ are the joints positions, velocities, and accelerations, respectively; $M(q) \in \mathbb{R}^{n\times n}$ is the non-singular inertia matrix; $C(q,\dot{q}) \in \mathbb{R}^{n\times n}$ is the Coriolis and centrifugal matrix; $G(q) \in \mathbb{R}^n$ represent the gravity forces vector; $F(\dot{q}) \in \mathbb{R}^n$ is the dissipation term; $\tau_{exo} \in \mathbb{R}^n$ and $\tau_{hum} \in \mathbb{R}^n$ are the exoskeleton and human torques, respectively; $u \in \mathbb{R}^n$ is the control signal input.

The dynamic model of the system 4.1 can be written as

$$\ddot{q} = f(q,\dot{q}) + g(q)\,u + d(t) \tag{4.2}$$

where $f(q,\dot{q})$, $g(q)$ and $d(t)$ are given by

$$f(q,\dot{q}) = -M(q)^{-1}\,H(q,\dot{q})$$

$$g(q) = M(q)^{-1}$$

$$d(t) = M(q)^{-1}\,\tau_{hum}$$

where $d(t) \in \mathbb{R}^n$ is considered as the unknown uncertainties and external bounded disturbances vector, which will be compensated by the controller.

The following assumptions are considered:

Assumption 1: The positions $q(t)$ and the velocities $\dot{q}(t)$ are measured.

Assumption 2: The disturbance $d(t)$ is differentiable with respect to time and its derivative $\dot{d}(t)$ is bounded.

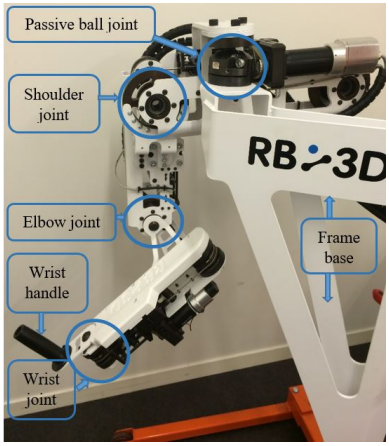

(a) *ULEL prototype.*

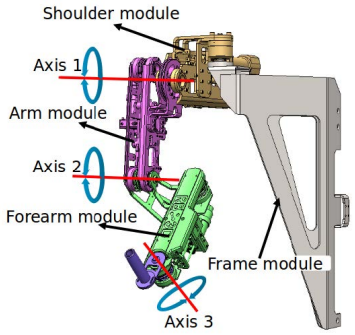

(b) *Permitted CAD model.*

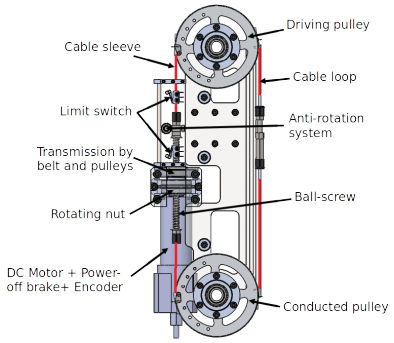

(c) *Shoulder CAD model.*

Figure 4.1: *Mechanical structure of ULEL.*

4.3 Adaptive super twisting sliding mode controller

In this study, the Adaptive ST-SMC (AST-SMC) is employed to address the limitations of the classical super twisting algorithm, particularly its need for frequent parameter adaptation for each user. The decision to use a second-order controller like the ST-SMC algorithm over alternatives such as classical SMC or PID is based on its demonstrated superiority in robustness and reliability, which includes several advantages:

- Ensuring high-quality trajectory tracking in both position and velocity
- Capable of achieving equilibrium within finite time for both the sliding surface and its derivative
- Effectively and smoothly eliminating external disturbances within finite time
- Providing comfort and safety for the wearer.

This section details the controller design and introduces an online adaptation PSO-based algorithm. The stability analysis and proof of finite-time convergence of the proposed controller are presented in appendix 4.5.

4.3.1 Controller design

The control law has been structured into two steps: initially choosing the sliding surface, followed by the subsequent design of the controller.

Let the sliding surface of the super twisting controller be defined as:

$$S = \dot{e} + \lambda e \tag{4.3}$$

where $S^T = [S_1, ..., S_n] \in \mathbb{R}^n$ is the sliding manifold, $\lambda \in \mathbb{R}$ is a positive constant; $e, \dot{e} \in \mathbb{R}^n$ are the joint position and velocity errors, respectively, such $e = q_d - q$ and $\dot{e} = \dot{q}_d - \dot{q}$ with $q_d, \dot{q}_d \in \mathbb{R}^n$ are the desired position and velocity joints separately.

Remark: In order to achieve exponential convergence of the error dynamics within the sliding mode ($S = 0$), it has been determined that the constant λ should be positive.

The proposed AST-SMC, derived from references [182,183], is formulated as follows:

$$u = g\,(q)^{-1}\left(\ddot{q}_d - f\,(q, \dot{q}) + \lambda\,\dot{e} + K_1\sqrt{|S|}sign\,(S) + \int K_2 sign\,(S)\,dt\right) \tag{4.4}$$

where $K_1 = diag\left(K_{1,1}, ..., K_{1,n}\right) \in \mathbb{R}^{n\times n}$ and $K_2 = diag\left(K_{2,1}, ..., K_{2,n}\right) \in \mathbb{R}^{n\times n}$ the controller's parameters which are constrained within bounds defined in the proof section section 4.5, and they will be optimized using the PSO algorithm detailed in section 4.3.2 and illustrated in Figure 4.2, these parameters are formed by positive diagonal matrices. $\sqrt{|S|}$ is a matrix such $\sqrt{|S|} = diag\left(\sqrt{|S_1|}, ..., \sqrt{|S_n|}\right) \in \mathbb{R}^{n\times n}$; whereas $sign\,(S)$ is a vector such $sign\,(S) = [sign\,(S_1)\,, ..., sign\,(S_n)]^T \in \mathbb{R}^n$ and $\ddot{q}_d \in \mathbb{R}^n$ is the desired acceleration.

Substituting the control law 4.4 into the Equation 4.2 gives:

$$\begin{aligned}\ddot{q} &= f\,(q, \dot{q}) + g\,(q)\,u + d(t)\\ &= \ddot{q}_d + \lambda\,\dot{e} + K_1\sqrt{|S|}\,sign\,(S) + \int K_2\,sign\,(S)\,dt + d(t)\end{aligned}$$

Then it comes:

$$\ddot{q}_d - \ddot{q} + \lambda\,\dot{e} + K_1\sqrt{|S|}\,sign\,(S) + \int K_2\,sign\,(S)\,dt + d(t) = 0 \tag{4.5}$$

Since the derivative of the sliding surface S is given by $\dot{S} = (\ddot{q}_d - \ddot{q} + \lambda\,\dot{e})$ then the Equation 4.5 can be written the following Super Twisting (ST) form:

$$\dot{S} = -K_1\,\sqrt{|S|}\,sign\,(S) - \int K_2\,sign\,(S)\,dt - d(t) \tag{4.6}$$

The Equation 4.6 can still be written in the following system:

$$\begin{cases}\dot{S} = -K_1\,\sqrt{|S|}\,sign\,(S) + Z\\ \dot{Z} = -K_2\,sign\,(S) - \dot{d}(t)\end{cases} \tag{4.7}$$

A recall of the Lyapunov stability analysis of the ST algorithm is given in the Appendix 4.5. Therefore, the system 4.7 which represents the closed loop dynamics is stable and its finite-time convergence is guaranteed.

4.3.2 PSO algorithm

Because the super twisting algorithm contains many parameters, selecting a meta-heuristic algorithm like PSO to optimize their eigenvalues is an effective method to enhance and adapt any controller. However, the evaluation criteria must be thoroughly studied and tailored to the specific application. The custom PSO algorithm applied in this work is adopted from [184], with the relevant Equations provided below.

$$V_i^{j+1} = w^j V_i^j + c_1 \left(P_i^j - X_i^j\right) + c_2 \left(G^j - X_i^j\right) + c_3 \frac{r^j}{||V_i^j||^2} \tag{4.8}$$

$$X_i^{j+1} = X_i^j + V_i^{j+1} \tag{4.9}$$

where j the iteration and

- c_1, c_2, $c_3 \in \mathbb{R}$ are positive constants.
- $r^j \in \mathbb{R}^m$ is a random positive vector at the iteration j.
- $P_i^j \in \mathbb{R}^m$ is the personal best vector of the i-th particle at the iteration j.
- $G^j \in \mathbb{R}^m$ is the global best vector of all particles at the iteration j.
- X_i^j, $X_i^{j+1} \in \mathbb{R}^m$ are the current and updated position vectors separately of the i-th particle.
- V_i^j, $V_i^{j+1} \in \mathbb{R}^m$ are the current and updated velocity vectors, respectively of the i-th particle.
- $w^j \in \mathbb{R}$ is a positive weigh computed by

$$w^j = w_{max} - \left(\frac{(w_{max} - w_{min})}{j_{max}}\right) \times j \tag{4.10}$$

where w_{min} and w_{max} are the minimal and the maximal value and j_{max} is the maximal value of the iteration j.

The parameters are calculated using the following Equation:

$$\theta(t + dt) = \theta(t) + G^{j_{max}}$$

where dt is the sampling time, $\theta(t) = [K_{1,1}(t), ..., K_{1,n}(t), K_{2,1}(t), ..., K_{2,n}(t)]^T \in \mathbb{R}^{2n}$ is the parameter vector at the moment t and $G^{j_{max}} \in \mathbb{R}^m$ is the global best vector of all particles at the final iteration j_{max}.

Before defining the objective function, lets introduce the following hypothesis.

Assumption 3: *Let $T \in \mathbb{R}^+$ be a short period of time such $u(t)$ and $\ddot{q}(t)$ remain constants for $t \in [t, t + T]$.*

The Equation of motion will be defined by

$$\dot{q}(t + T) = \ddot{q}(t) T + \dot{q}(t) \tag{4.11}$$

and

$$q\left(t+T\right)=\frac{1}{2}\ddot{q}\left(t\right)T^{2}+\dot{q}\left(t\right)T+q\left(t\right) \tag{4.12}$$

The objective function employed in this thesis incorporates the norms of the predictive sliding surface $S\left(t+T\right)$, the control signal $u\left(t\right)$, and the swarm position $X(t)$ to prevent high gains and minimize power consumption. It is defined as follows:

$$J=\alpha\left\|S\left(t+T\right)\right\|+\beta\left\|u\left(t\right)\right\|+\gamma\left\|X(t)\right\| \tag{4.13}$$

with

$$S\left(t+T\right)=\left(\dot{q}_{d}\left(t+T\right)-\dot{q}\left(t+T\right)\right)+\lambda\left(q_{d}\left(t+T\right)-q\left(t+T\right)\right) \tag{4.14}$$

where $t\in\mathbb{R}$ is the current time; α, β, $\gamma\in\mathbb{R}$ are positive constant scalars.

A summary of the PSO algorithm optimization is presented in Table 4.1. Additionally, the control diagram of the newly proposed controller is depicted in Figure 4.2.

Table 4.1: *PSO Algorithm.*

1. Set parameters ranges
2. Initialize the swarm
3. Particles initial assessment
4. Select the initial global best
5. Loop {Iteration = max}
{
a. Update velocity and position
b. Check the limits
c. Evaluate the particles
d. Update the global best
}
6. Save positions and velocities
7. Take the global best as the optimal solution
8. Calculate the real parameters ($K_1$and K_2)
9. Verify upper and lower limits

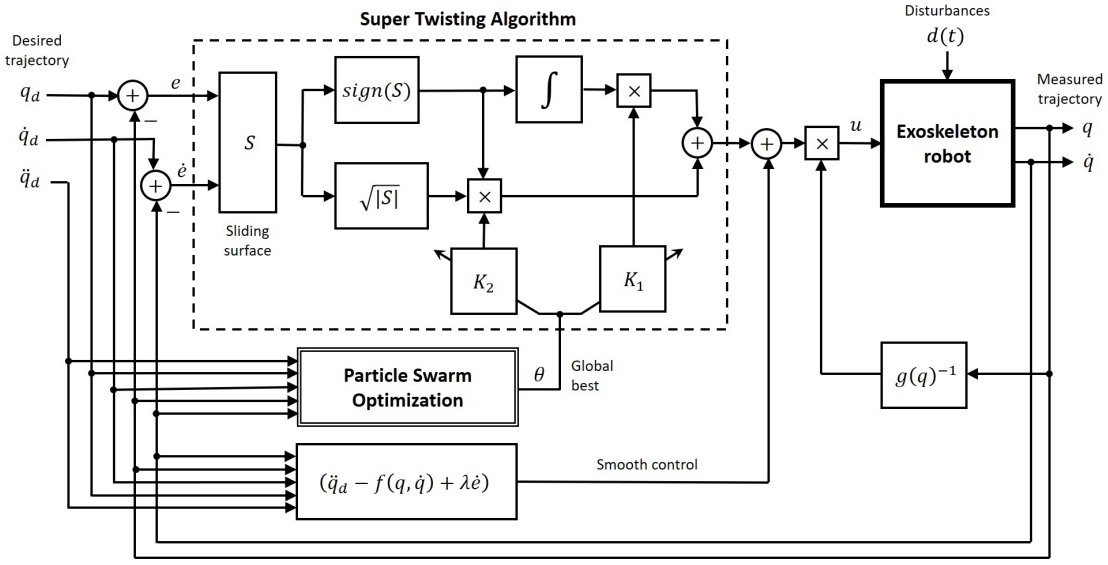

Figure 4.2: *Controller diagram.*

4.4 Results and analysis

To verify and validate the performance of the proposed online adaptive controller, both simulations and real-time experiments were conducted on the ULEL robot, which is a 3 DoF right upper limb exoskeleton robot. This exoskeleton, which was designed by RB3D for arm rehabilitation, has the mechanical characteristics detailed in Tables 2.1 and 2.2. The tests conducted for this study focused solely on the 2 DoF of the shoulder and elbow, allowing for flexion/extension movements. The parameter values used for the PSO are summarized in Table 4.2.

Table 4.2: *Parameters values.*

Parameter	Eigenvalue
Particle position	$random \in [0, 1]$
Particle velocity	0
Iteration	10
Population	20
w_{max}	1.7
w_{min}	0.4
c_1	0.7
c_2	0.3
c_3	10^{-8}
α	0.001
β	8
γ	5
λ	3

4.4.1 Simulation results

Initially, simulations were conducted using the dynamic model of the exoskeleton outlined in Chapter 2. To assess the robustness of the proposed approach, sinusoidal resistive and assistive external disturbance forces were applied in software, depicted in Figure 4.5 and described by Equation 4.15. These forces represent assistive and resistive rehabilitation therapies, respectively, where the patient initially remains passive during the early stages of therapy. After a certain period, the patient is encouraged to either resist or assist the robot to enhance brain control recovery. The amplitudes of these disturbances exceed 20% of the maximum applied torques on both joints. A comparison between the proposed AST-SMC control law and the classical ST-SMC algorithm is presented to demonstrate the performance of the proposed controller.

$$\begin{aligned} d_1(t) &= \begin{cases} -5\ \sin\left(0.5\,t - \frac{\pi}{2}\right) & \text{if } t \in [20, 40] \\ +5\ \sin\left(0.5\,t - \frac{\pi}{2}\right) & \text{if } t \in [60, 80] \\ 0 & \text{otherwise} \end{cases} \\ d_2(t) &= \begin{cases} -2\ \sin\left(0.7\,t + \frac{\pi}{2}\right) & \text{if } t \in [20, 40] \\ +2\ \sin\left(0.7\,t + \frac{\pi}{2}\right) & \text{if } t \in [60, 80] \\ 0 & \text{otherwise} \end{cases} \end{aligned} \tag{4.15}$$

The classical super twisting control law, as described in section 4.4, is identical to the adaptive version, with the exception of its non-adaptive parameters (fixed) K_1 and K_2.

$$K_1 = \begin{bmatrix} 6 & 0 \\ 0 & 4 \end{bmatrix}, K_2 = \begin{bmatrix} 6 & 0 \\ 0 & 4 \end{bmatrix}$$

The desired trajectories that have been used are sinusoidal and expressed as the following:

$$\begin{cases} q_{d1}(t) = \frac{\pi}{10}\ \sin\left(0.5t - \frac{\pi}{2}\right) + \frac{\pi}{6} \\ q_{d2}(t) = \frac{\pi}{10}\ \sin\left(0.7t + \frac{\pi}{2}\right) + \frac{\pi}{6} \end{cases} \tag{4.16}$$

Discussion:

Figure 4.3 demonstrates the minimization of the objective function and its convergence to nearly zero, indicating that the optimal parameters have been found. In other words, the figure illustrates the effectiveness of the PSO algorithm in identifying the appropriate eigenvalues required for the controller.

Figure 4.4 illustrates the behavior of the controller parameters during the online search. Despite initializing parameters K_1 and K_2 with random values within the ranges $[1-5]$ and $[1-3]$, respectively, the proposed technique successfully converges to the optimal values, as shown in the figure. However, starting with better initial values would accelerate the convergence to the optimal parameters. Although K_1' and K_2' began with poor initial guesses, leading to relatively suboptimal tracking performance, Figure 4.3 demonstrates their eventual convergence to the optimal values.

For joint position trajectory tracking, Figures 4.6 and 4.7 illustrate the tracking position and its associated error. These figures highlight the superior performance of the proposed

controller compared to the classical ST-SMC, particularly in terms of trajectory tracking and robustness against external disturbances. Specifically, at moments 20s and 80s, the error of the classical controller is almost double that of the proposed one for the shoulder joint, confirming the proposed controller's efficiency.

The joint velocity trajectory tracking is depicted in Figures 4.8 and 4.9, demonstrating the performance of the proposed approach. The start and end moments of the external disturbances further emphasize the efficiency of the proposed adaptive controller compared to other controllers.

Figure 4.10 shows the torques applied to the shoulder and elbow joints. Despite the presence of resistive and assistive perturbations, the proposed PSO algorithm enables the controller to generate adequate and optimal torques.

The Root Mean Square (RMS) of the steady-state tracking errors in position and velocity is illustrated in Figure 4.11. This figure demonstrates the effectiveness of the proposed adaptive controller over the classical ST-SMC, even though the parameters of the classical ST-SMC algorithm were carefully chosen.

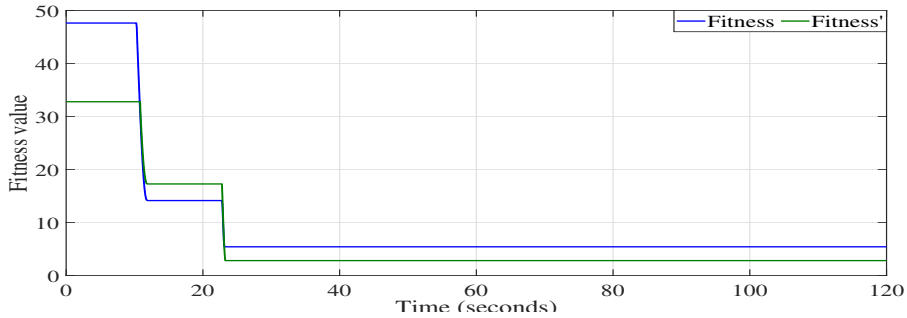

Figure 4.3: *Evolution of the objective function*

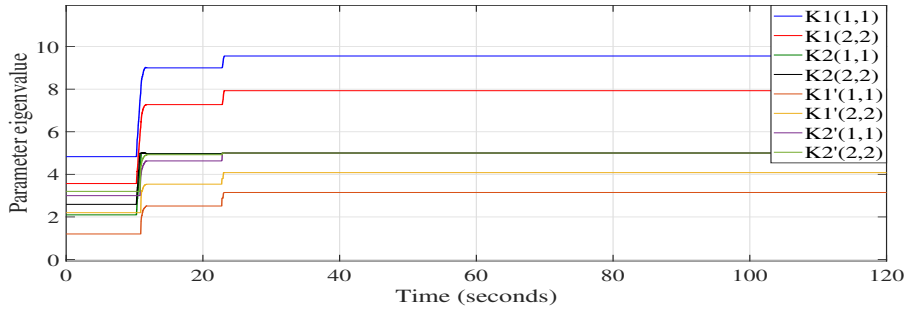

Figure 4.4: *Controller parameters obtained with PSO in good K and bad K′ initial* guesses *cases.*

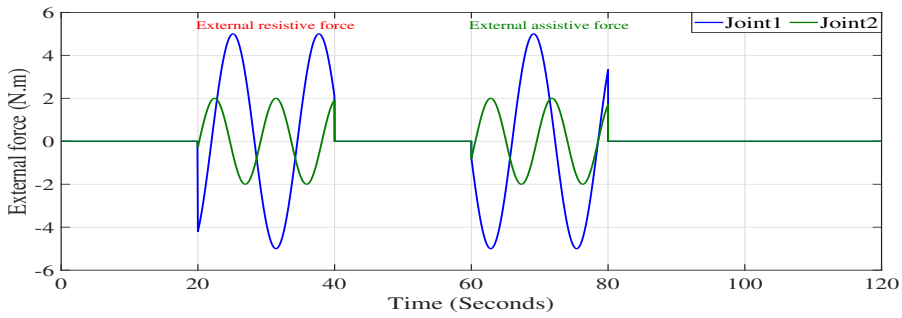

Figure 4.5: *External disturbances efforts applied on joint 1 and 2*

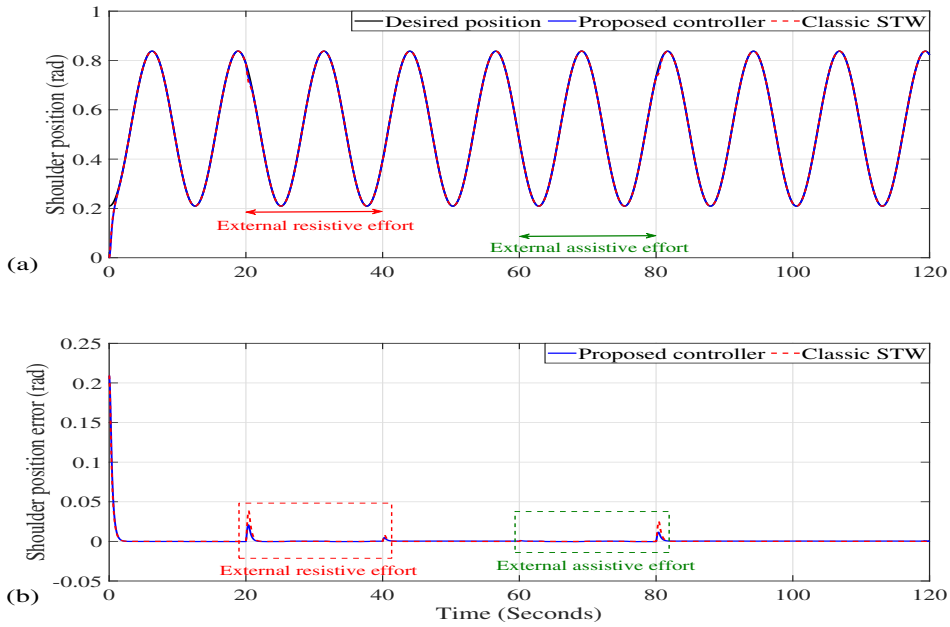

Figure 4.6: *Position trajectory tracking of joint 1 of the proposed controller AST-SMC and classic ST-SMC, respectively: (a) Position trajectory tracking; (b) Position tracking error.*

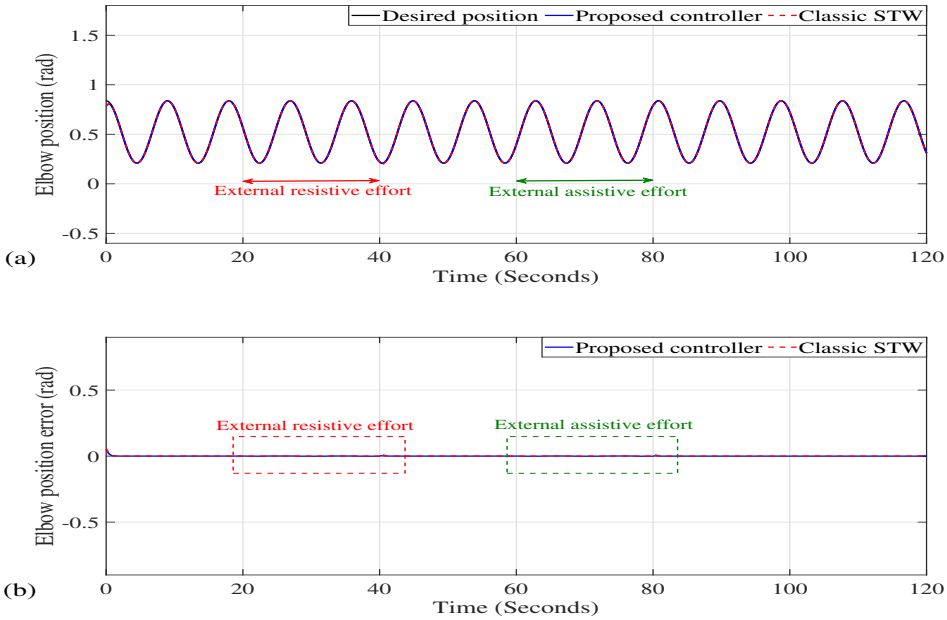

Figure 4.7: *Position trajectory tracking of joint 2 of the proposed controller AST-SMC and classic ST-SMC, respectively: (a) Position trajectory tracking; (b) Position tracking error.*

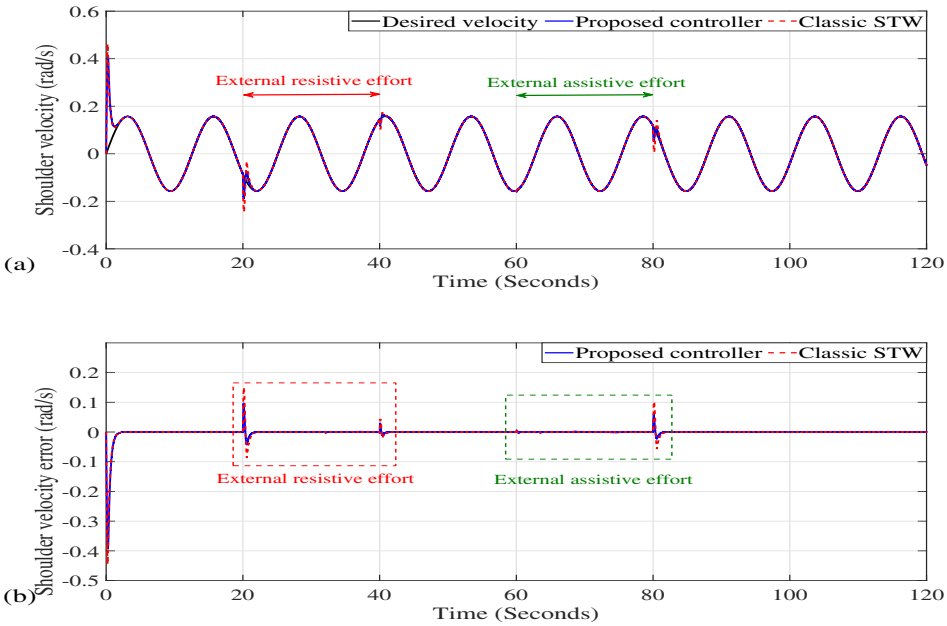

Figure 4.8: *Velocity trajectory tracking of joint 1 of the proposed controller AST-SMC and classic ST-SMC, respectively: (a) Velocity trajectory tracking; (b) Velocity tracking error.*

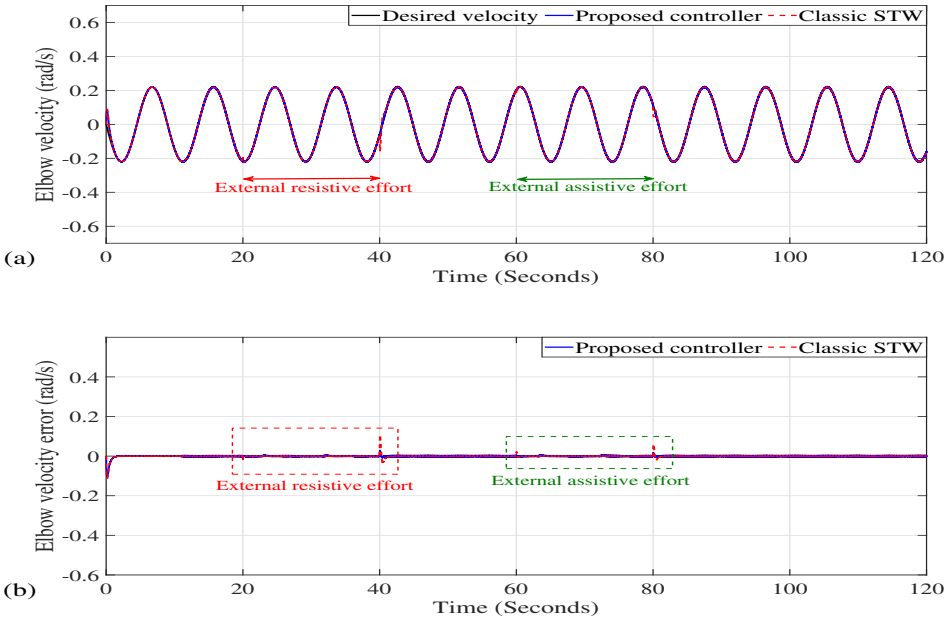

Figure 4.9: *Velocity trajectory tracking of joint 2 of the proposed controller AST-SMC and classic ST-SMC, respectively: (a) Velocity trajectory tracking; (b) Velocity tracking error.*

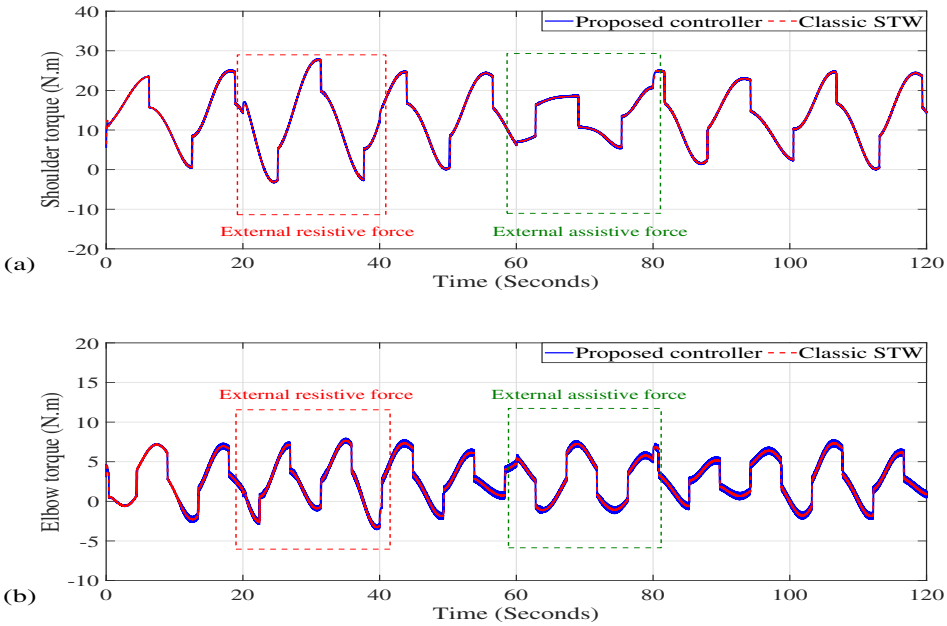

Figure 4.10: *Input control torques for joints 1 and 2 with external disturbances: (a) Represent joint 1; (b) Represent joint 2.*

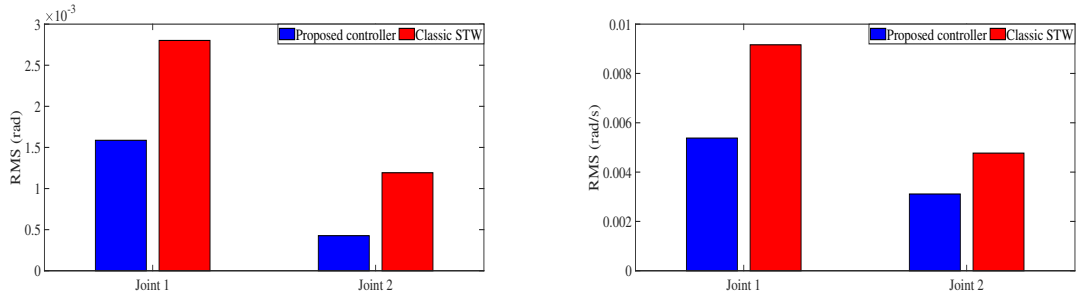

(a) *Position tracking error.* (b) *Velocity tracking error.*

Figure 4.11: *Position and velocity tracking error RMS.*

4.4.2 Experimental results

Experiment validation was conducted to verify the effectiveness of the proposed adaptive controller. The exoskeleton actuators use current-controlled DC motors from MAXON. Encoders measure the real position of each joint. Safety requirements, including limit switches, current limits, and mechanical stops, were considered and activated during the experiments. A first-order Euler solver with a sufficiently small sampling time of 0.004s was used. The experimental setup, shown in Figure 4.12, is based on a computer equipped with a dSpace DS1103 PPC real-time controller card and MATLAB/Simulink software with the dSpace control desk application.

Before starting experiments with a real subject, the following safety protocol was implemented:

1. Conducting test runs without a subject.
2. Adjusting mechanical stops to prevent unwanted positions.
3. Setting electrical current limits for the actuators' motors to bound the applied torques.
4. Ensuring emergency stop buttons are always accessible near the handle.

- Experimental Scenarios

Tests were initially conducted on the ULEL exoskeleton without any wearer, followed by experiments with two subjects detailed in Table 4.3.

During the tests, the subjects were instructed to:

1. Remain completely passive without applying any resistive or assistive efforts:

$\tau_{hum} = 0.$

1. Exert an assisting muscular effort: $\tau_{hum} \neq 0$ in the same direction as τ_{exo}, and a resistive muscular effort: $\tau_{hum} \neq 0$ in the opposite direction of τ_{exo} during specific time intervals.

Discussion:

Figures 4.13 and 4.14 demonstrate sustained trajectory tracking in position for both joints 1 and 2. Although human subjects were instructed to remain completely passive, this is not entirely feasible in practice. Notably, during the intervals [40 - 60] seconds and [100 - 120] seconds, the subjects were not completely passive. Even with this lack of passiveness, the error remains negligible, highlighting the quality and efficiency of the proposed controller.

Figures 4.15 and 4.16 illustrate the trajectory tracking in velocity for both joints 1 and 2. These figures show the effectiveness of the proposed controller in achieving the desired velocity in the presence of measurement noise.

The control inputs shown in Figure 4.17 depict the efforts applied by the controller on the actuators and clearly illustrate the impact of the subjects on the control torques. Although the varying sizes and weights of the wearers, the proposed controller generates smooth torques for each subject.

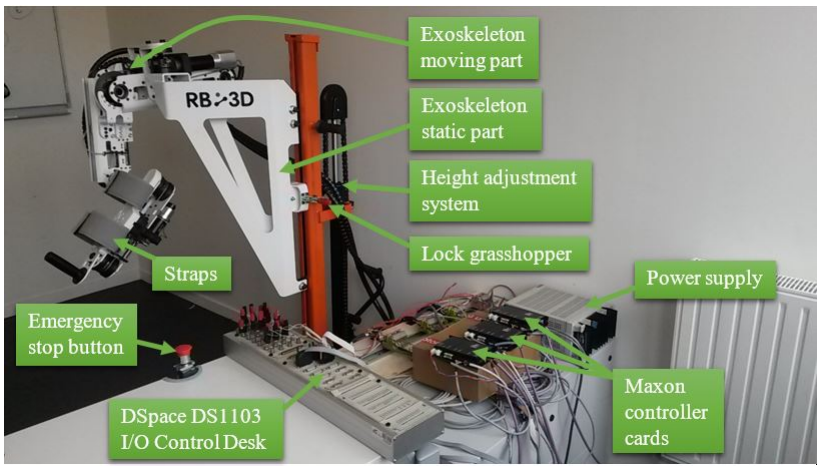

Figure 4.12: *Experimental setup.*

Table 4.3: *Subjects used in experiments*

Subjects	No 1	No 2
Sex	Male	Male
Age (year)	46	16
Weight (Kg)	67	78
Height (m)	1.65	1.79

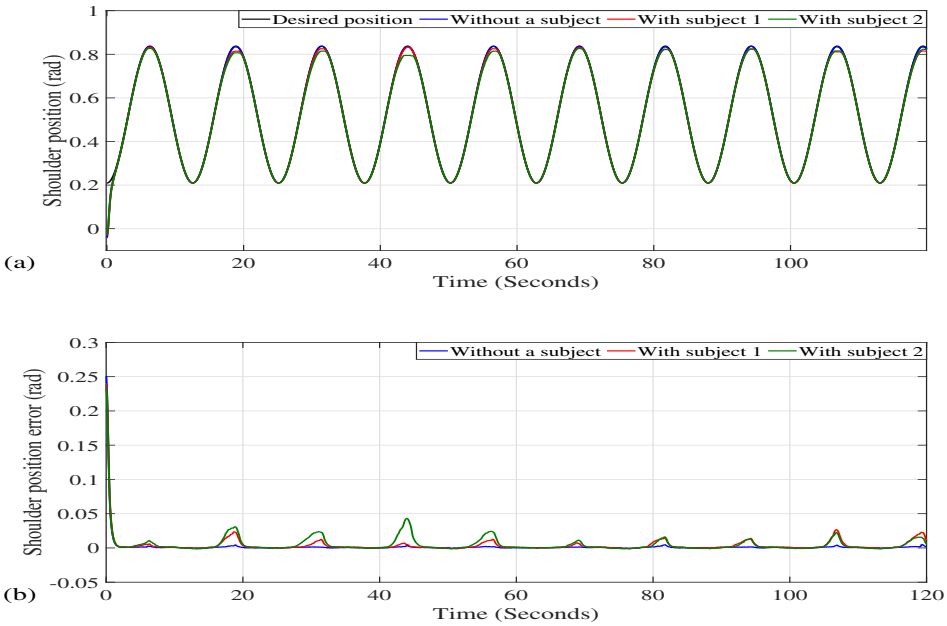

Figure 4.13: *Position trajectory tracking of joint 1, trial without a subject and with subjects 1 and 2: (a) Position trajectory tracking; (b) Position tracking error.*

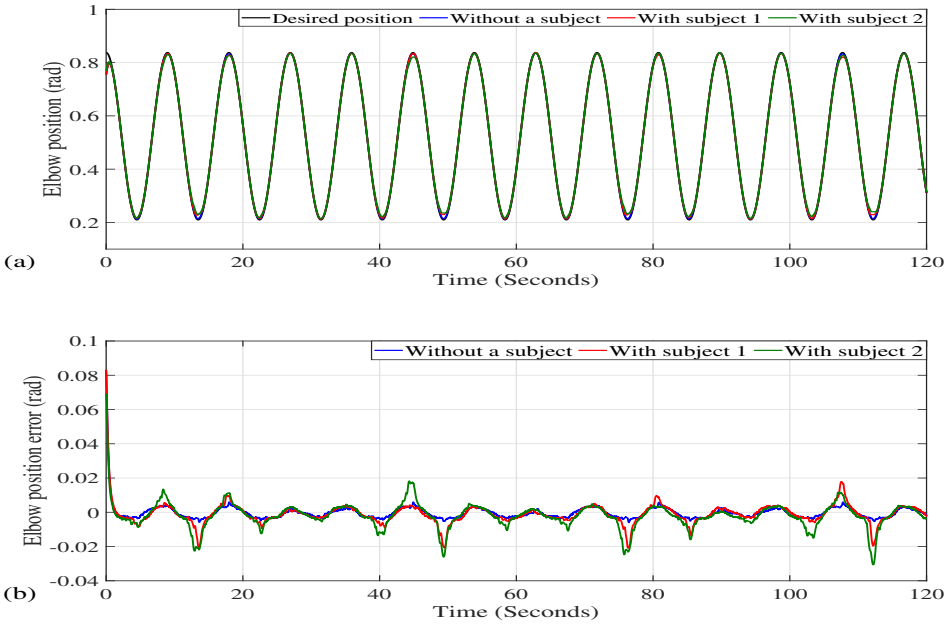

Figure 4.14: *Position trajectory tracking of joint 2, trial without a subject and with subjects 1 and 2: (a) Position trajectory tracking; (b) Position tracking error.*

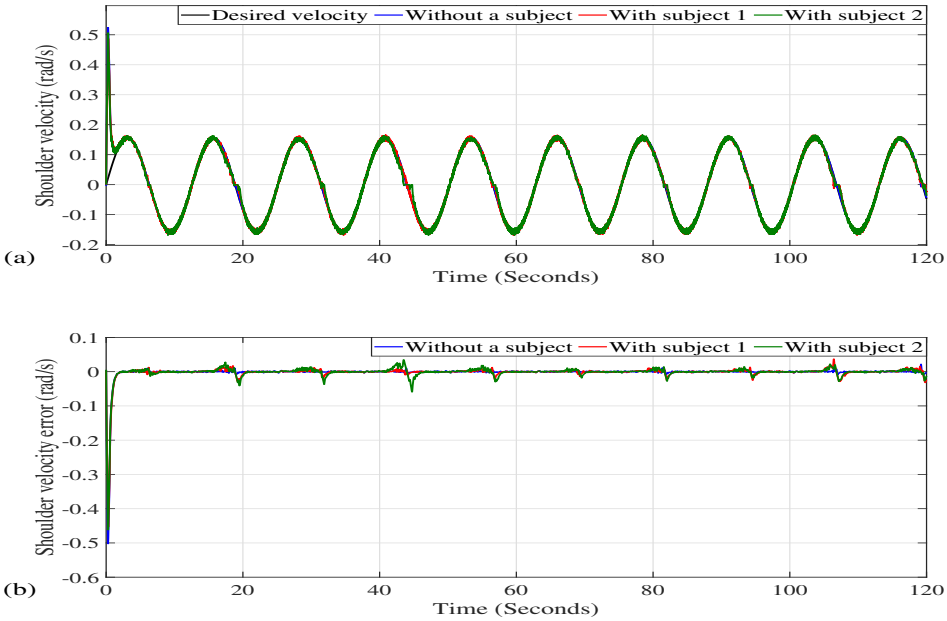

Figure 4.15: *Velocity trajectory tracking of joint 1, trial without a subject and with subjects 1 and 2: (a) Position trajectory tracking; (b) Position tracking error.*

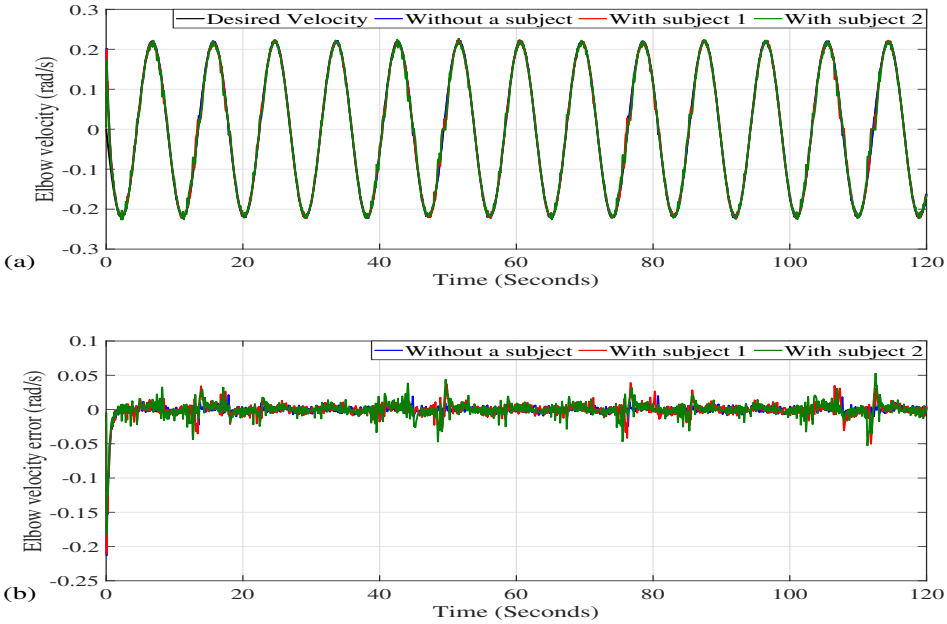

Figure 4.16: *Position trajectory tracking of joint 2, trial without a subject and with subjects 1 and 2: (a) Position trajectory tracking; (b) Position tracking error.*

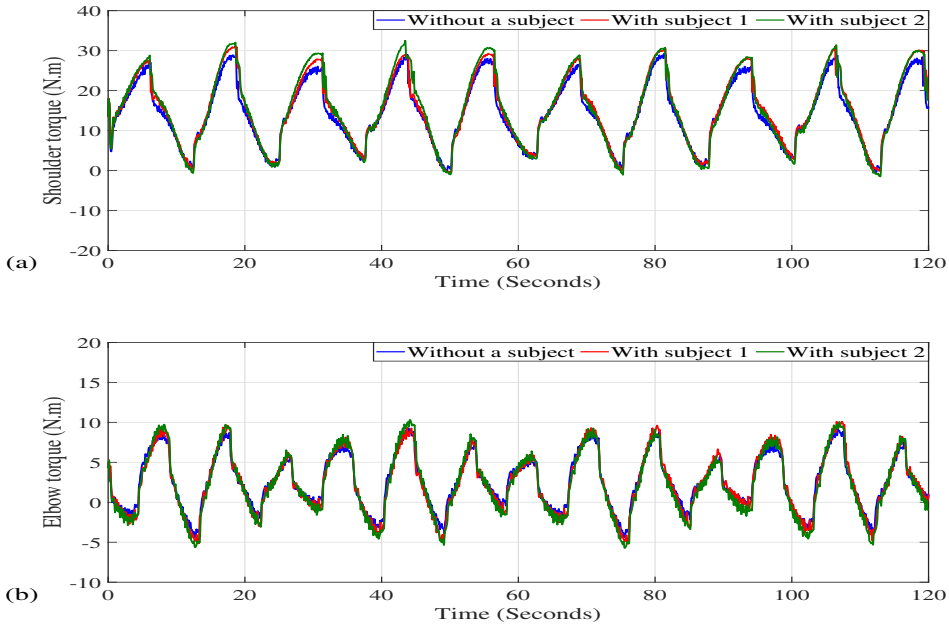

Figure 4.17: *Input control torques for joints 1 and 2 without any external perturbations: (a) Represent joint 1; (b) Represent joint 2.*

Since the controller has been applied to two joints (shoulder and elbow), it is challenging for the wearers to exert identical external resistive and assistive efforts on both articulations simultaneously. As a result, the impact of external disturbances on the applied torques, shown in Figure 4.22, might be unclear. However, this impact is evident in the position and velocity trajectory tracking.

Figures 4.18 and 4.19 show the position trajectory tracking of joints 1 and 2 in the presence of external disturbances. Despite the strong perturbation forces, especially in joint 2, the proposed controller remains stable and maintains smooth position trajectory tracking.

Figures 4.20 and 4.21 illustrate the velocity trajectory tracking of joints 1 and 2 under external disturbances. It is evident that the proposed controller effectively handles external disturbances of varying amplitudes, highlighting its performance.

Figure 4.22 displays the generated torques in joints 1 and 2 for each subject. These results show that the proposed controller responded consistently with the test subjects. Additionally, the interactions with the exoskeleton varied between the wearers, yet the controller maintained smooth torques. This demonstrates the optimization of the torques in conjunction with the controller parameters, proving the efficiency and performance of the proposed controller.

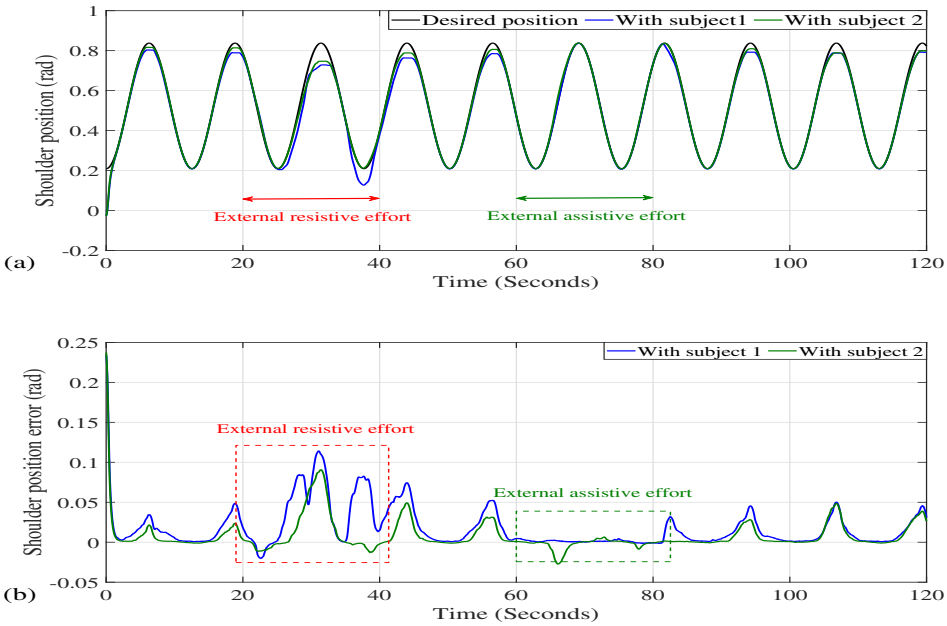

Figure 4.18: *Position trajectory tracking of joint 1 with the presence of disturbances, trial with subjects 1 and 2: (a) Position trajectory tracking; (b) Position tracking error.*

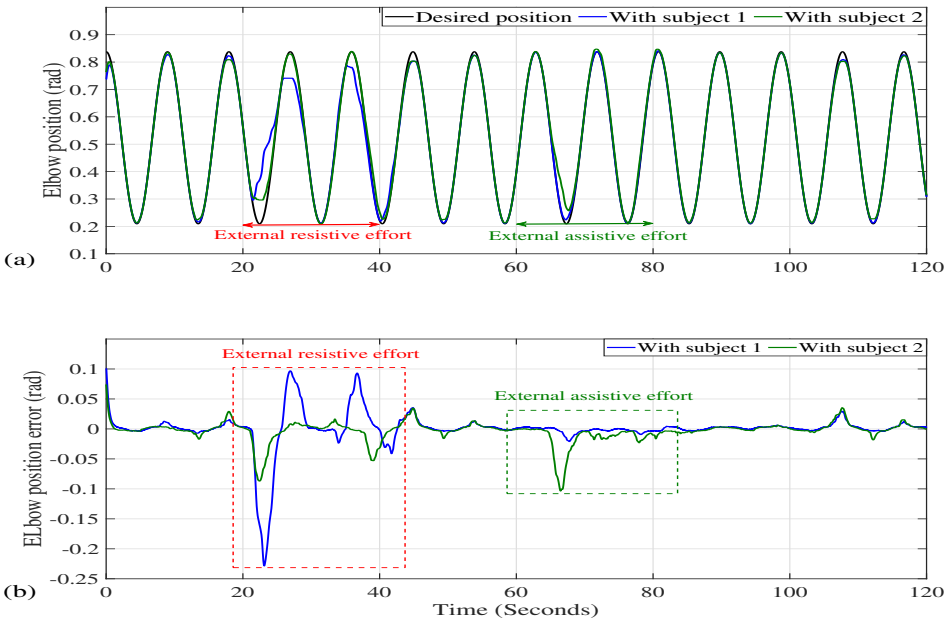

Figure 4.19: *Position trajectory tracking of joint 2 with the presence of disturbances, trial with subjects 1 and 2: (a) Position trajectory tracking; (b) Position tracking error.*

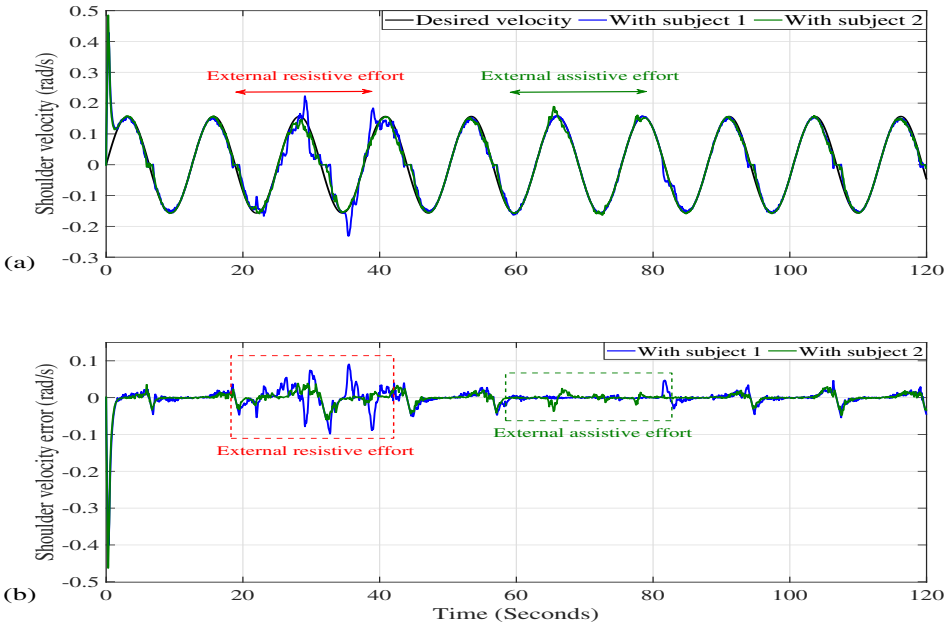

Figure 4.20: *Velocity trajectory tracking of joint 1 with the presence of disturbances, trial with subjects 1 and 2: (a) Position trajectory tracking; (b) Position tracking error.*

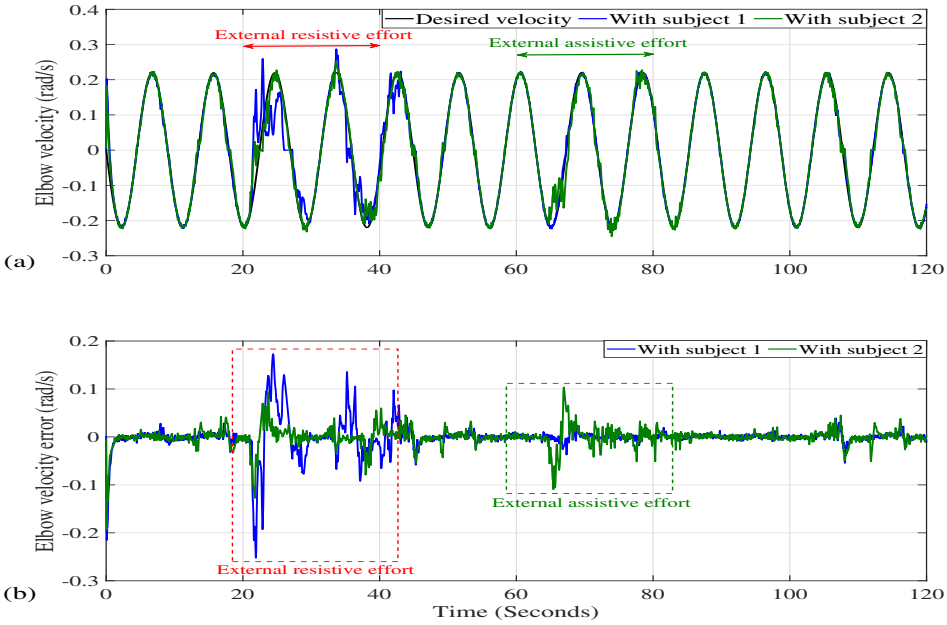

Figure 4.21: *Velocity trajectory tracking of joint 2 with the presence of disturbances, trial with subjects 1 and 2: (a) Position trajectory tracking; (b) Position tracking error.*

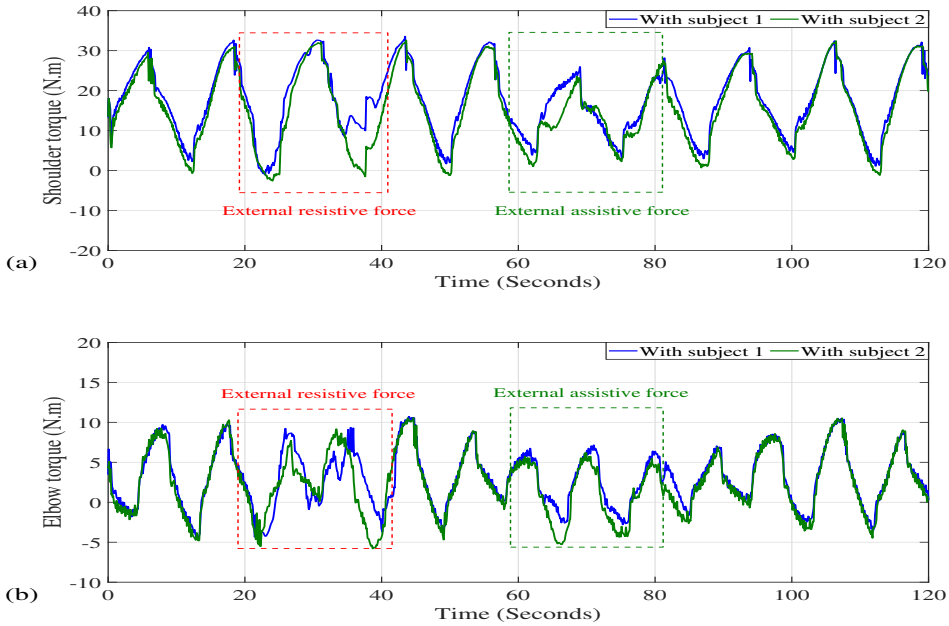

Figure 4.22: *Input control torques for joints 1 and 2 with the presence of external disturbances: (a) Represent joint 1; (b) Represent joint 2.*

4.5 Conclusion

In this chapter, a real-time adaptive controller is introduced for an upper limb exoskeleton rehabilitation robot. This approach utilizes the Super-Twisting algorithm, with its parameters computed through a novel online PSO algorithm. The novelty of the proposed technique lies in formulating the optimization criterion's cost function. Moreover, adaptation focuses on optimizing parameter variations rather than the parameters themselves. The algorithm's parameters are dynamically adjusted based on closed-loop stability analysis conditions.

The effectiveness of this approach has been evaluated through simulations and real-life experiments involving two healthy subjects. Simulation results demonstrate the superiority of the proposed controller over classical method. Consequently, experiments exclusively utilized the proposed controller under two scenarios: subjects remaining passive or exerting external resistive/assistive forces.

The satisfactory experimental outcomes within rehabilitation contexts validate the effectiveness of the proposed approach. They highlight its robustness against external disturbances, contrasting with previous studies employing offline or non-adaptive controllers.

Conclusion:

This doctoral thesis focuses on the development of a novel control algorithm for a portable exoskeleton robot designed to facilitate upper limb rehabilitation. The exoskeleton is available at the LISSI laboratory in France and has been specifically engineered to support and enhance the rehabilitation process by accurately replicating natural arm movements. The control algorithm was developed to ensure that the exoskeleton could adapt to real-time changes and maintain stability and precision.

A comprehensive review of existing exoskeleton technologies was conducted, encompassing a variety of exoskeletons and their applications across diverse fields. This state-of-the-art review provided a robust foundation for comprehending the extant technological landscape and identified avenues for enhancement. Subsequently, a comprehensive modeling of the exoskeleton's dynamics was performed. This was a critical step in the design of an efficient control law, as precise models facilitate the accurate tailoring of control strategies for the exoskeleton robot.

An in-depth study of the PSO algorithm was conducted to examine its potential in refining control parameters for exoskeletons. Indeed, the third chapter delves deeply into the PSO algorithm, detailing its mechanics and how it can be effectively applied to optimize the performance of a control system. By simulating various scenarios and adjusting the control parameters through PSO, the research showed an improved efficiency and adaptability of the exoskeleton's control algorithm. This optimization process was the key to enhance the overall functionality of the exoskeleton, ensuring that it can reliably assist with upper limb rehabilitation under diverse conditions.

The efficacy of the newly developed control algorithm was evaluated through both simulation and experimental testing on two healthy subjects. The experimental validation involved three distinct scenarios: passive movement (no effort from the wearer), cooperative movement (the wearer and exoskeleton work in unison), and resistive movement (the wearer resists the exoskeleton). The results exhibits excellent performance in all scenarios, with the algorithm maintaining accurate trajectory tracking and robust performance against external disturbances.

The findings from this research were published in a renowned scientific journal, highlighting the significance of this new control approach in the field of medical robotics. The successful implementation and validation of the algorithm underscore its potential to enhance the effectiveness of exoskeleton-assisted rehabilitation.

Future research directions include integrating intelligent control strategies based on user intentions (EMG) and incorporating impedance control to better manage the interaction forces between the wearer and the exoskeleton. These advancements aim to make the exoskeleton more intuitive and responsive, ultimately improving the rehabilitation experi-

ence for users.

Appendix:

A.1 Lyapunov stability analysis of the Super-Twisting algorithm

Consider the standard Super-Twisting algorithm (ST) with a perturbation term

$$\begin{cases} \dot{\sigma}_1 = -k_1\sqrt{|\sigma_1|}sign\,(\sigma_1) + \sigma_2 \\ \dot{\sigma}_2 = -k_2\,sign\,(\sigma_1) + \xi(t,\sigma) \end{cases} \tag{A1}$$

where $\sigma_1, \sigma_2 \in \mathbb{R}$ and the perturbation term ξ is uniformly bounded ($|\xi| < \delta$).

Let us prove the stability of the equilibrium point $(\sigma_1, \sigma_2) = (0, 0)$ using the work stated in [185, 186].

Consider the following Lyapunov function:

$$V = \zeta^T P \zeta \tag{A2}$$

where $\zeta = [\sqrt{|\sigma_1|}sign\,(\sigma_1)\,, \sigma_2]^T$ and P is a positive definite matrix.

Notice that $V(\zeta, t)$ is continuous and differentiable except when $\sigma_1 = 0$.In fact, when $\sigma_1 \neq 0$, $\dot{V}$ exists and is negative definite. However, before arriving at the equilibrium point $(\sigma_1, \sigma_2) = (0, 0)$, the solution of system A1 crosses the line $\sigma_1 = 0$ when $\sigma_2 \neq 0$. This means that the derivative of the Lyapunov function exists almost everywhere while $V(t)$ decreases until the system reaches the equilibrium. As presented in [186],$V(t)$ is a strong Lyapunov funtion for Equation A1 in the form of Equation A2.

Moreover, this Lyapunov function is positive definite but radially unbouneded

$$\gamma_{min}(P)\,\|\zeta\|^2 \leq V \leq \gamma_{max}(P)\,\|\zeta\|^2 \tag{A3}$$

where $\|\zeta\|_2^2 = |\sigma_1| + \sigma_2^2$ represents the Euclidian norm of ζ.

The construction of suitable positive definite matrices $P = P^T$, provided in [186], is based on the following algebraic LMI Equation:

$$\begin{bmatrix} A^T P + PA + \epsilon P + \delta^2 C^T C & PB \\ B^T P & -1 \end{bmatrix} < 0 \tag{A4}$$

where

$$A = \begin{bmatrix} -\frac{1}{2}k_1 & \frac{1}{2} \\ -k_2 & 0 \end{bmatrix}; B = \begin{bmatrix} 0 \\ 1 \end{bmatrix}; C = \begin{bmatrix} 1 & 0 \end{bmatrix}$$

with $k_1$and k_2 are postive gains.

Using the vector $\zeta = [\sqrt{|\sigma_1|}sign\,(\sigma_1)\,, \sigma_2]^T$, the system A1 can be rewritten as

$$\dot{\zeta} = \frac{1}{|\zeta_1|}(A\zeta + B\tilde{\xi}(t)) \tag{A5}$$

where the transformed perturbation $\tilde{\xi}(t, \zeta) = |\zeta_1|\,\xi(t, \sigma)$ satisfies $\left|\tilde{\xi}(t, \zeta)\right| \leq \delta\,|\xi_1|$. As a consequence, $\omega(\tilde{\xi}, \zeta) = -\tilde{\xi}^2(t, \zeta) + \delta^2\zeta_1^2 \geq 0$.

As $k_1$and k_2 are positive gains, the system (A,B,C) is observable and controllable, so we can use the bounded-real [187]. It is shown that the Linear Matrix Inequality A4 is feasable if and only if the inear system defined by $H(s) = \delta C(sI - A)^{-1}B$ is nonexpansive, i.e.

$$\max_{\omega} |H(j\omega)| < 1$$

This implies the following condition:

$$\max_{\omega} |G(j\omega)| < \frac{1}{\delta}$$

where

$$G(s) = C(sI - A)^{-1}B = \frac{\frac{1}{2}}{s^2 + \frac{1}{2}k_1 s + \frac{1}{2}k_2}$$

The previous equality yields to two conditions on gains. By choosing one of them

$$\max_{\omega} |G(j\omega)| = \frac{1}{k_2} if\, k_1^2 > 4k_2$$

We can then deduce conditions on gains $k_1$and $k_2$as follows:

$$\begin{gathered} k_2 > \delta \\ k_1^2 > 4k_2 \end{gathered}$$

Consider the Lyapunov function defined by Equation A2. Its derivative writes

$$\begin{aligned} \dot{V}(\zeta) &= \tfrac{1}{|\zeta_1|}\left[\zeta\tilde{\xi}\right]^T \begin{bmatrix} A^TP + PA & PB \\ B^TP & 0 \end{bmatrix} \left[\zeta\tilde{\xi}\right] \\ &\leq \tfrac{1}{|\zeta_1|}\left\{\left[\zeta\tilde{\xi}\right]^T \begin{bmatrix} A^TP + PA & PB \\ B^TP & 0 \end{bmatrix} \left[\zeta\tilde{\xi}\right] + \omega(\tilde{\xi},\zeta)\right\} \\ &\leq \tfrac{1}{|\zeta_1|}\left[\zeta\tilde{\xi}\right]^T \begin{bmatrix} A^TP + PA + \delta^2C^TC & PB \\ B^TP & -1 \end{bmatrix} \left[\zeta\tilde{\xi}\right] \\ &\leq \tfrac{1}{|\zeta_1|}\left[\zeta\tilde{\xi}\right]^T \begin{bmatrix} A^TP + PA + \epsilon P - \epsilon P + \delta^2C^TC & PB \\ B^TP & -1 \end{bmatrix} \left[\zeta\tilde{\xi}\right] \\ &\leq -\tfrac{\epsilon}{|\zeta_1|}\zeta^TP\zeta \end{aligned}$$

Finally

$$\dot{V} \leq -\frac{\epsilon}{|\zeta_1|}\zeta^TP\zeta = -\frac{\epsilon}{|\zeta_1|}V(\zeta) \tag{A6}$$

From Equation A3, we deduce the following inequality:

$$|\zeta_1| \leq \|\zeta\|_2 \leq \frac{V^{1/2}(\zeta)}{\gamma_{min}^{1/2}\{P\}}$$

We can then conclude that $\dot{V}$satisfies

$$\dot{V} \leq -\alpha V^{1/2}(\zeta)$$

where

$$\alpha = \epsilon\gamma_{min}^{1/2}\{P\} \tag{A7}$$

The previous result guarantees the finite convergence of vector $\sigma = [\sigma_1, \sigma_2]^T$ to zero. This time is bounded by

$$T_0 = \frac{2V^{1/2}(\zeta(0))}{\alpha} \tag{A8}$$

where $\zeta(0)$ is the initial value of ζ and α is given by Equation A7.

Bibliography

[1] A. Jebri, T. Madani, K. Djouani, A. Benallegue, Robust adaptive neuronal controller for exoskeletons with sliding-mode, Neurocomputing 399 (2020) 317–330.

[2] A. Jellali, T. Madani, N. Khraief, S. Belghith, Non-singular terminal sliding mode controller in cartesian space: Application to an upper limb exoskeleton, in: 2023 21st International Conference on Advanced Robotics (ICAR), IEEE, 2023, pp. 558–563.

[3] A. Riani, T. Madani, A. Benallegue, K. Djouani, Adaptive integral terminal sliding mode control for upper-limb rehabilitation exoskeleton, Control Engineering Practice 75 (2018) 108–117.

[4] M. Daachi, T. Madani, B. Daachi, K. Djouani, A radial basis function neural network adaptive controller to drive a powered lower limb knee joint orthosis, Applied Soft Computing 34 (2015) 324–336.

[5] G. Onose, V. Cârdei, Ş. T. Crăciunoiu, V. Avramescu, I. Opriş, M. A. Lebedev, M. V. Constantinescu, Mechatronic wearable exoskeletons for bionic bipedal standing and walking: a new synthetic approach, Frontiers in neuroscience 10 (2016) 343.

[6] E. Carmeli, S. Peleg, G. Bartur, E. Elbo, J. Vatine, Handtutor enhanced hand rehabilitation after stroke a pilot study, Physiotherapy Research International 16 (2011) 191–200.

[7] M. Nilsson, J. Ingvast, J. Wikander, H. von Holst, The soft extra muscle system for improving the grasping capability in neurological rehabilitation, in: 2012 IEEE-EMBS conference on biomedical engineering and sciences, IEEE, 2012, pp. 412–417.

[8] S. Kim, M. A. Nussbaum, M. I. M. Esfahani, M. M. Alemi, B. Jia, E. Rashedi, Assessing the influence of a passive, upper extremity exoskeletal vest for tasks requiring arm elevation: Part ii unexpected effects on shoulder motion, balance, and spine loading, Applied Ergonomics 70 (2018) 323–330.

[9] N. Norouzi-Gheidari, P. S. Archambault, J. Fung, Effects of robot-assisted therapy on stroke rehabilitation in upper limbs: Systematic review and meta-analysis of the literature, The Journal of Rehabilitation Research and Development 49 (2012) 479.

[10] S. Mendis, Stroke disability and rehabilitation of stroke: World health organization perspective, International Journal of Stroke 8 (2013) 3–4.

[11] H. S. Lo, S. Q. Xie, Exoskeleton robots for upper-limb rehabilitation: State of the art and future prospects, Medical Engineering Physics 34 (2012) 261–268.

[12] A. Frisoli, C. Procopio, C. Chisari, I. Creatini, L. Bonfiglio, M. Bergamasco, B. Rossi, M. Carboncini, Positive effects of robotic exoskeleton training of upper limb reaching movements after stroke, Journal of NeuroEngineering and Rehabilitation 9 (2012) 36.

[13] P. H. I. Groshaw, Arm test, hardiman i prototype, general electric rep, Tech. rep., Technical report S-70-1019.

[14] S. Christensen, S. Bai, Kinematic analysis and design of a novel shoulder exoskeleton using a double parallelogram linkage, Journal of Mechanisms and Robotics 10 (4) (2018) 041008.

[15] M. Bianchi, F. Fanelli, R. Conti, L. Governi, E. Meli, A. Ridolfi, A. Rindi, F. Vannetti, B. Allotta, Design and motion analysis of a wearable and portable hand exoskeleton, in: Wearable Robotics: Challenges and Trends: Proceedings of the 2nd International Symposium on Wearable Robotics, WeRob2016, October 18-21, 2016, Segovia, Spain, Springer, 2017, pp. 373–377.

[16] B. Kim, A. D. Deshpande, An upper-body rehabilitation exoskeleton harmony with an anatomical shoulder mechanism: Design, modeling, control, and performance evaluation, The International Journal of Robotics Research 36 (2017) 414–435.

[17] G. Bao, L. Pan, H. Fang, X. Wu, H. Yu, S. Cai, B. Yu, Y. Wan, Academic review and perspectives on robotic exoskeletons, IEEE Transactions on Neural Systems and Rehabilitation Engineering 27 (2019) 2294–2304.

[18] N. Rehmat, J. Zuo, W. Meng, Q. Liu, S. Q. Xie, H. Liang, Upper limb rehabilitation using robotic exoskeleton systems: a systematic review, International Journal of Intelligent Robotics and Applications 2 (2018) 283–295.

[19] R. Bertani, C. Melegari, M. C. De Cola, A. Bramanti, P. Bramanti, R. S. Calabrò, Effects of robot-assisted upper limb rehabilitation in stroke patients: a systematic review with meta-analysis, Neurological Sciences 38 (2017) 1561–1569.

[20] M. Mekki, A. D. Delgado, A. Fry, D. Putrino, V. Huang, Robotic rehabilitation and spinal cord injury: a narrative review, Neurotherapeutics 15 (2018) 604–617.

[21] K. E. Gordon, G. S. Sawicki, D. P. Ferris, Mechanical performance of artificial pneumatic muscles to power an ankleâfoot orthosis, Journal of Biomechanics 39 (2006) 1832–1841.

[22] J. Stein, K. Narendran, J. McBean, K. Krebs, R. Hughes, Electromyography-controlled exoskeletal upper-limbâpowered orthosis for exercise training after stroke, American Journal of Physical Medicine Rehabilitation 86 (2007) 255–261.

[23] C. J. WALSH, K. ENDO, H. HERR, A quasi-passive leg exoskeleton for load-carrying augmentation, International Journal of Humanoid Robotics 04 (2007) 487–506.

[24] M. Fontana, R. Vertechy, S. Marcheschi, F. Salsedo, M. Bergamasco, The body extender: A full-body exoskeleton for the transport and handling of heavy loads, IEEE Robotics Automation Magazine 21 (2014) 34–44.

[25] M. B. Näf, A. S. Koopman, S. Baltrusch, C. Rodriguez-Guerrero, B. Vanderborght, D. Lefeber, Passive back support exoskeleton improves range of motion using flexible beams, Frontiers in Robotics and AI 5 (2018) 72.

[26] J. J. Knapik, K. L. Reynolds, E. Harman, Soldier load carriage: Historical, physiological, biomechanical, and medical aspects, Military Medicine 169 (2004) 45–56.

[27] T. Du Plessis, K. Djouani, C. Oosthuizen, A review of active hand exoskeletons for rehabilitation and assistance, Robotics 10 (1) (2021) 40.

[28] H. F. Al-Shuka, M. H. Rahman, S. Leonhardt, I. Ciobanu, M. Berteanu, Biomechanics, actuation, and multi-level control strategies of power-augmentation lower extremity exoskeletons: An overview, International Journal of Dynamics and Control 7 (2019) 1462–1488.

[29] F. Hussain, R. Goecke, M. Mohammadian, Exoskeleton robots for lower limb assistance: A review of materials, actuation, and manufacturing methods, Proceedings of the Institution of Mechanical Engineers, Part H: Journal of Engineering in Medicine 235 (12) (2021) 1375–1385.

[30] S. Jatsun, A. Malchikov, O. Loktionova, A. Yatsun, Modeling of human-machine interaction in an industrial exoskeleton control system, in: Interactive Collaborative Robotics: 5th International Conference, ICR 2020, St Petersburg, Russia, October 7-9, 2020, Proceedings 5, Springer, 2020, pp. 116–125.

[31] K. Xia, X. Chen, X. Chang, C. Liu, L. Guo, X. Xu, F. Lv, Y. Wang, H. Sun, J. Zhou, Hand exoskeleton design and human–machine interaction strategies for rehabilitation, Bioengineering 9 (11) (2022) 682.

[32] A. Singla, S. Dhand, A. Dhawad, G. S. Virk, Toward human-powered lower limb exoskeletons: A review, Harmony Search and Nature Inspired Optimization Algorithms: Theory and Applications, ICHSA 2018 (2019) 783–795.

[33] L. Wang, Z. Fei, Y. Qi, C. Zhang, L. Zhao, Z. Jiang, R. Maeda, Overview of human kinetic energy harvesting and application, ACS Applied Energy Materials 5 (6) (2022) 7091–7114.

[34] A. Plaza, M. Hernandez, G. Puyuelo, E. Garces, E. Garcia, Wearable rehabilitation exoskeletons of the lower limb: analysis of versatility and adaptability, Disability and Rehabilitation: Assistive Technology 18 (2023) 392–406.

[35] U. Onen, F. M. Botsali, M. Kalyoncu, M. Tinkir, N. Yilmaz, Y. Sahin, Design and actuator selection of a lower extremity exoskeleton, IEEE/ASME Transactions on Mechatronics 19 (2014) 623–632.

[36] D. S. Pina, A. A. Fernandes, R. N. Jorge, J. Gabriel, Designing the mechanical frame of an active exoskeleton for gait assistance, Advances in Mechanical Engineering 10 (2) (2018) 1687814017743664.

[37] H. Cao, Z. Ling, J. Zhu, Y. Wang, W. Wang, Design frame of a leg exoskeleton for load-carrying augmentation, in: 2009 IEEE international conference on robotics and biomimetics (ROBIO), IEEE, 2009, pp. 426–431.

[38] C. Di Natali, S. Toxiri, S. Ioakeimidis, D. G. Caldwell, J. Ortiz, Systematic framework for performance evaluation of exoskeleton actuators, Wearable Technologies 1 (2020) e4.

[39] J. M. Font-Llagunes, U. Lugrís, D. Clos, F. J. Alonso, J. Cuadrado, Design, control, and pilot study of a lightweight and modular robotic exoskeleton for walking assistance after spinal cord injury, journal of Mechanisms and Robotics 12 (3) (2020) 031008.

[40] C. D. Natali, S. Toxiri, S. Ioakeimidis, D. G. Caldwell, J. Ortiz, Systematic framework for performance evaluation of exoskeleton actuators, Wearable Technologies 1 (2020) e4.

[41] M. Tiboni, A. Borboni, F. Vérité, C. Bregoli, C. Amici, Sensors and actuation technologies in exoskeletons: A review, Sensors 22 (3) (2022) 884.

[42] Y. Yao, D. Shao, M. Tarabini, S. A. Moezi, K. Li, P. Saccomandi, Advancements in sensor technologies and control strategies for lower-limb rehabilitation exoskeletons: A comprehensive review, Micromachines 15 (4) (2024) 489.

[43] D. Copaci, D. Serrano, L. Moreno, D. Blanco, A high-level control algorithm based on semg signalling for an elbow joint sma exoskeleton, Sensors 18 (2018) 2522.

[44] A. Kapsalyamov, S. Hussain, P. K. Jamwal, State-of-the-art assistive powered upper limb exoskeletons for elderly, IEEE Access 8 (2020) 178991–179001.

[45] R. Gopura, D. Bandara, K. Kiguchi, G. Mann, Developments in hardware systems of active upper-limb exoskeleton robots: A review, Robotics and Autonomous Systems 75 (2016) 203–220.

[46] J. Rosen, J. C. Perry, Upper limb powered exoskeleton, International Journal of Humanoid Robotics 4 (03) (2007) 529–548.

[47] E. B. Weston, M. Alizadeh, H. Hani, G. G. Knapik, R. A. Souchereau, W. S. Marras, A physiological and biomechanical investigation of three passive upper-extremity exoskeletons during simulated overhead work, Ergonomics 65 (2022) 105–117.

[48] K. Huysamen, T. Bosch, M. de Looze, K. S. Stadler, E. Graf, L. W. O'Sullivan, Evaluation of a passive exoskeleton for static upper limb activities, Applied Ergonomics 70 (2018) 148–155.

[49] S. K. Manna, V. N. Dubey, Comparative study of actuation systems for portable upper limb exoskeletons, Medical Engineering Physics 60 (2018) 1–13.

[50] M. Tröster, D. Wagner, F. Müller-Graf, C. Maufroy, U. Schneider, T. Bauernhansl, Biomechanical model-based development of an active occupational upper-limb exoskeleton to support healthcare workers in the surgery waiting room, International Journal of Environmental Research and Public Health 17 (14) (2020) 5140.

[51] A. Blanco, J. M. Catalan, D. Martinez, J. V. Garcia-Perez, N. Garcia-Aracil, The effect of an active upper-limb exoskeleton on metabolic parameters and muscle activity during a repetitive industrial task, IEEE Access 10 (2022) 16479–16488.

[52] S. Christensen, S. Rafique, S. Bai, Design of a powered full-body exoskeleton for physical assistance of elderly people, International Journal of Advanced Robotic Systems 18 (6) (2021) 17298814211053534.

[53] R. P. Matthew, E. J. Mica, W. Meinhold, J. A. Loeza, M. Tomizuka, R. Bajcsy, Introduction and initial exploration of an active/passive exoskeleton framework for portable assistance, in: 2015 IEEE/RSJ International Conference on Intelligent Robots and Systems (IROS), IEEE, 2015, pp. 5351–5356.

[54] L. Grazi, E. Trigili, G. Proface, F. Giovacchini, S. Crea, N. Vitiello, Design and experimental evaluation of a semi-passive upper-limb exoskeleton for workers with motorized tuning of assistance, IEEE Transactions on Neural Systems and Rehabilitation Engineering 28 (2020) 2276–2285.

[55] G. Zeilig, H. Weingarden, M. Zwecker, I. Dudkiewicz, A. Bloch, A. Esquenazi, Safety and tolerance of the rewalk exoskeleton suit for ambulation by people with complete spinal cord injury: A pilot study, The Journal of Spinal Cord Medicine 35 (2012) 96–101.

[56] V. Lajeunesse, C. Vincent, F. Routhier, E. Careau, F. Michaud, Exoskeletons' design and usefulness evidence according to a systematic review of lower limb exoskeletons used for functional mobility by people with spinal cord injury, Disability and Rehabilitation: Assistive Technology 11 (2016) 535–547.

[57] E. Høyer, A. Opheim, V. Jørgensen, Implementing the exoskeleton ekso gttm for gait rehabilitation in a stroke unit–feasibility, functional benefits and patient experiences, Disability and Rehabilitation: Assistive Technology 17 (4) (2022) 473–479.

[58] A. Riani, Control and observation of exoskeletons for upper limb functional rehabilitation., Ph.D. thesis, University of Paris-Saclay, France (2018).

[59] M. P. De Looze, T. Bosch, F. Krause, K. S. Stadler, L. W. Oâsullivan, Exoskeletons for industrial application and their potential effects on physical work load, Ergonomics 59 (5) (2016) 671–681.

[60] L. Serebrennikova, Development and assessment of the army exoskeleton, Ph.D. thesis, WORCESTER POLYTECHNIC INSTITUTE (2023).

[61] B. Watson, Onyx exoskeleton: An inside look at lockheed martin's wearable robot. (3 2020).
URL https://www.ucf.edu/pegasus/power-move-onyx-exoskeleton/

[62] Krishna, Raytheon xos 2 exoskeleton, second-generation robotics suit. (6 2020).
URL https://www.army-technology.com/projects/raytheonxos-2-exoskeleton-us/

[63] F. Valagussa, N. Biliouris, A. Strickland, L. Reid, L. Serebrennikova, R. Hendrick, Development and assessment of the army exoskeleton (4 2023).
URL https://digital.wpi.edu/concern/student_works/zc77st32m?locale=pt-BR

[64] Mxo, Uprisetm load-bearing exoskeleton | mawashi (Feb. 2024).
URL https://mawashi.ca/en/defence-and-security/uprise/

[65] A. Wall, J. Borg, S. Palmcrantz, Clinical application of the hybrid assistive limb (hal) for gait trainingâa systematic review, Frontiers in systems neuroscience 9 (2015) 48.

[66] A. Kapsalyamov, P. K. Jamwal, S. Hussain, M. H. Ghayesh, State of the art lower limb robotic exoskeletons for elderly assistance, IEEE Access 7 (2019) 95075–95086.

[67] B. Chen, Y. Zhou, C. Chen, Z. Sayeed, J. Hu, J. Qi, T. Frush, H. Goitz, J. Hovorka, M. Cheng, C. Palacio, Volitional control of upper-limb exoskeleton empowered by emg sensors and machine learning computing, Array 17 (2023) 100277.

[68] V. Varma, R. Y. Rao, P. Vundavilli, M. Pandit, P. Budarapu, A machine learning-based approach for the design of lower limb exoskeleton, International Journal of Computational Methods 19 (08) (2022) 2142012.

[69] Y. Codex, Review of control systems for optimizing exoskeleton performance: Integrating machine learning and sensor technologies (10 2023).
URL https://codex.yubetsu.com/article/0f66fade45f84ad0a81fa16e891097a7

[70] J. Li, C. Chen, Machine learning-based energy harvesting for wearable exoskeleton robots, Sustainable Energy Technologies and Assessments 57 (2023) 103122.

[71] A. F. P. Vidal, J. Y. R. Morales, G. O. Torres, F. de Jesus Sorcia Vazquez, A. C. Rojas, J. A. B. Mendoza, J. C. R. Cerda, Soft exoskeletons: Development, requirements, and challenges of the last decade, Actuators 10 (2021) 166.

[72] L. Randazzo, Neuroprosthetics to support impaired hand functions: A multidisciplinary approach combining brain-machine interfaces and wearable exoskeletons (2018) 115.
URL http://infoscience.epfl.ch/record/260469

[73] M. Sharbafi, A. Naseri, A. Seyfarth, M. Grimmer, Neural control in prostheses and exoskeletons, Elsevier, 2020, pp. 153–178.

[74] O. El-Edrissi, Contribution of an upper body stick-figure model for subject-specific scaling approaches of generic musculoskeletal models in the anybody modelling system, Ph.D. thesis (07 2020).

[75] B. TONDU, A kinematic model of the upper limb with a clavicle-like link for humanoid robots, International Journal of Humanoid Robotics 05 (2008) 87–118.

[76] P. M. Ludewig, V. Phadke, J. P. Braman, D. R. Hassett, C. J. Cieminski, R. F. LaPrade, Motion of the shoulder complex during multiplanar humeral elevation, The Journal of Bone and Joint Surgery-American Volume 91 (2009) 378–389.

[77] C. Neu, J. Crisco, S. Wolfe, In vivo kinematic behavior of the radio-capitate joint during wrist flexion extension and radio-ulnar deviation, Journal of Biomechanics 34 (2001) 1429–1438.

[78] U. K. Latif, Z. Gong, V. Nanjappan, G. V. Georgiev, Designing for rehabilitation movement recognition and measurement in virtual reality, Proceedings of the Design Society 3 (2023) 1387–1396.

[79] P. Garrec, Screw and nut transmission and cable attached to the screw, uS Patent 7,073,406 (Jul. 11 2006).
URL https://patents.google.com/patent/US7073406B2/en

[80] W. Khalil, E. Dombre, Modeling identification and control of robots, CRC Press, 2002.

[81] Z. Yang, W. Gu, J. Zhang, L. Gui, Force Control Theory and Method of Human Load Carrying Exoskeleton Suit, Springer Berlin Heidelberg, 2017.

[82] B. S. R. Armstrong, Dynamics for robot control: friction modeling and ensuring excitation during parameter identification, Stanford University, 1988.

[83] B. Armstrong-Hélouvry, P. Dupont, C. C. De Wit, A survey of models, analysis tools and compensation methods for the control of machines with friction, Automatica 30 (7) (1994) 1083–1138.

[84] L. Gaul, R. Nitsche, The role of friction in mechanical joints, American Society of Mechanical Engineers, Applied Mechanics Reviews 54 (2001) 93–106.

[85] J. Kennedy, R. Eberhart, Particle swarm optimization, in: Proceedings of ICNN'95-international conference on neural networks, Vol. 4, ieee, 1995, pp. 1942–1948.

[86] M. Imran, R. Hashim, N. E. A. Khalid, An overview of particle swarm optimization variants, Procedia Engineering 53 (2013) 491–496.

[87] N. Q. Uy, N. X. Hoai, R. McKay, P. M. Tuan, Initialising pso with randomised low-discrepancy sequences: the comparative results, IEEE, 2007, pp. 1985–1992.

[88] H. Jabeen, Z. Jalil, A. R. Baig, Opposition based initialization in particle swarm optimization (o-pso), ACM, 2009, pp. 2047–2052.

[89] M. Pant, R. Thangaraj, C. Grosan, A. Abraham, Improved particle swarm optimization with low-discrepancy sequences, in: 2008 IEEE congress on evolutionary computation (IEEE world congress on computational intelligence), IEEE, 2008, pp. 3011–3018.

[90] M. G. Omran, S. Al-Sharhan, Using opposition-based learning to improve the performance of particle swarm optimization, in: 2008 IEEE Swarm Intelligence Symposium, IEEE, 2008, pp. 1–6.

[91] C. Zhang, Z. Ni, Z. Wu, L. Gu, A novel swarm model with quasi-oppositional particle, in: 2009 International Forum on Information Technology and Applications, Vol. 1, IEEE, 2009, pp. 325–330.

[92] H.-R. Li, Y.-L. Gao, Particle swarm optimization algorithm with exponent decreasing inertia weight and stochastic mutation, in: 2009 second international conference on information and computing science, Vol. 1, IEEE, 2009, pp. 66–69.

[93] H. Wang, C. Li, Y. Liu, S. Zeng, A hybrid particle swarm algorithm with cauchy mutation, in: 2007 IEEE Swarm Intelligence Symposium, IEEE, 2007, pp. 356–360.

[94] H. Wang, H. Li, Y. Liu, C. Li, S. Zeng, Opposition-based particle swarm algorithm with cauchy mutation, in: 2007 IEEE congress on evolutionary computation, IEEE, 2007, pp. 4750–4756.

[95] M. Pant, R. Thangaraj, V. P. Singh, A. Abraham, Particle swarm optimization using sobol mutation, in: 2008 First International Conference on Emerging Trends in Engineering and Technology, IEEE, 2008, pp. 367–372.

[96] M. Imran, H. Jabeen, M. Ahmad, Q. Abbas, W. Bangyal, Opposition based pso and mutation operators, in: 2010 2nd International Conference on Education Technology and Computer, Vol. 4, IEEE, 2010, pp. V4–506.

[97] M. Imran, Z. Manzoor, S. Ali, Q. Abbas, Modified particle swarm optimization with student t mutation (stpso), in: International Conference on Computer Networks and Information Technology, IEEE, 2011, pp. 283–286.

[98] L. Chen, Particle swarm optimization with a novel mutation operator, in: 2011 International Conference on Mechatronic Science, Electric Engineering and Computer (MEC), IEEE, 2011, pp. 970–973.

[99] G. Pranava, P. Prasad, Constriction coefficient particle swarm optimization for economic load dispatch with valve point loading effects, in: 2013 international conference on power, energy and control (ICPEC), IEEE, 2013, pp. 350–354.

[100] S. A. Rather, P. S. Bala, Application of constriction coefficient-based particle swarm optimisation and gravitational search algorithm for solving practical engineering design problems, International Journal of Bio-Inspired Computation 17 (4) (2021) 246–259.

[101] S. A. Rather, P. S. Bala, Hybridization of constriction coefficient-based particle swarm optimization and chaotic gravitational search algorithm for solving engineering design problems, Applied Soft Computing and Communication Networks: Proceedings of ACN 2019 (2020) 95–115.

[102] H. Chongpeng, Z. Yuling, J. Dingguo, X. Baoguo, On some non-linear decreasing inertia weight strategies in particle swarm optimization, in: 2007 Chinese Control Conference, IEEE, 2007, pp. 750–753.

[103] Y. Shi, R. C. Eberhart, Fuzzy adaptive particle swarm optimization, in: Proceedings of the 2001 congress on evolutionary computation (IEEE Cat. No. 01TH8546), Vol. 1, IEEE, 2001, pp. 101–106.

[104] L. Zhang, H. Yu, S. Hu, A new approach to improve particle swarm optimization, in: Genetic and Evolutionary Computation Conference, Springer, 2003, pp. 134–139.

[105] J. Wei, Y. Wang, A dynamical particle swarm algorithm with dimension mutation, in: 2006 International Conference on Computational Intelligence and Security, Vol. 1, IEEE, 2006, pp. 254–257.

[106] M. Pant, T. Radha, V. Singh, Particle swarm optimization using gaussian inertia weight, in: International Conference on Computational Intelligence and Multimedia Applications (ICCIMA 2007), Vol. 1, IEEE, 2007, pp. 97–102.

[107] X. Liu, Q. Wang, H. Liu, L. Li, Particle swarm optimization with dynamic inertia weight and mutation, in: 2009 Third International Conference on Genetic and Evolutionary Computing, IEEE, 2009, pp. 620–623.

[108] V. Miranda, N. Fonseca, Epso-evolutionary particle swarm optimization, a new algorithm with applications in power systems, in: IEEE/PES transmission and distribution conference and exhibition, Vol. 2, IEEE, 2002, pp. 745–750.

[109] A. Esmin, G. Lambert-Torres, A. Z. de Souza, A hybrid particle swarm optimization applied to loss power minimization, IEEE Transactions on Power Systems 20 (2005) 859–866.

[110] M. Lovbjerg, T. K. Rasmussen, T. Krink, et al., Hybrid particle swarm optimiser with breeding and subpopulations, in: Proceedings of the genetic and evolutionary computation conference, Vol. 2001, San Francisco, USA, 2001, pp. 469–476.

[111] E. H. Houssein, A. G. Gad, K. Hussain, P. N. Suganthan, Major advances in particle swarm optimization: Theory, analysis, and application, Swarm and Evolutionary Computation 63 (2021) 100868.

[112] A. G. Gad, Particle swarm optimization algorithm and its applications: A systematic review, Archives of Computational Methods in Engineering 29 (2022) 2531–2561.

[113] E. Pashaei, E. Pashaei, N. Aydin, Gene selection using hybrid binary black hole algorithm and modified binary particle swarm optimization, Genomics 111 (2019) 669–686.

[114] N. Zeng, H. Qiu, Z. Wang, W. Liu, H. Zhang, Y. Li, A new switching-delayed-pso-based optimized svm algorithm for diagnosis of alzheimerâs disease, Neurocomputing 320 (2018) 195–202.

[115] I. Jain, V. K. Jain, R. Jain, Correlation feature selection based improved-binary particle swarm optimization for gene selection and cancer classification, Applied Soft Computing 62 (2018) 203–215.

[116] Y. Li, X. Bai, L. Jiao, Y. Xue, Partitioned-cooperative quantum-behaved particle swarm optimization based on multilevel thresholding applied to medical image segmentation, Applied Soft Computing 56 (2017) 345–356.

[117] S. Raj, K. C. Ray, Ecg signal analysis using dct-based dost and pso optimized svm, IEEE Transactions on Instrumentation and Measurement 66 (2017) 470–478.

[118] W. Srisukkham, L. Zhang, S. C. Neoh, S. Todryk, C. P. Lim, Intelligent leukaemia diagnosis with bare-bones pso based feature optimization, Applied Soft Computing 56 (2017) 405–419.

[119] S. Kumar, S. K. Pal, R. Singh, A novel hybrid model based on particle swarm optimisation and extreme learning machine for short-term temperature prediction using ambient sensors, Sustainable Cities and Society 49 (2019) 101601.

[120] A. Zarei, S.-F. Mousavi, M. E. Gordji, H. Karami, Optimal reservoir operation using bat and particle swarm algorithm and game theory based on optimal water allocation among consumers, Water Resources Management 33 (2019) 3071–3093.

[121] S. Chen, J. qiang Wang, H. yu Zhang, A hybrid pso-svm model based on clustering algorithm for short-term atmospheric pollutant concentration forecasting, Technological Forecasting and Social Change 146 (2019) 41–54.

[122] M. Rahgoshay, S. Feiznia, M. Arian, S. A. A. Hashemi, Simulation of daily suspended sediment load using an improved model of support vector machine and genetic algorithms and particle swarm, Arabian Journal of Geosciences 12 (2019) 277.

[123] V. P. Kour, S. Arora, Particle swarm optimization based support vector machine (p-svm) for the segmentation and classification of plants, IEEE Access 7 (2019) 29374–29385.

[124] Y. Cao, Y. Ye, H. Zhao, Y. Jiang, H. Wang, Y. Shang, J. Wang, Remote sensing of water quality based on hj-1a hsi imagery with modified discrete binary particle swarm optimization-partial least squares (mdbpso-pls) in inland waters: A case in weishan lake, Ecological Informatics 44 (2018) 21–32.

[125] M. A. Ghorbani, R. Kazempour, K.-W. Chau, S. Shamshirband, P. T. Ghazvinei, Forecasting pan evaporation with an integrated artificial neural network quantum-behaved particle swarm optimization model: a case study in talesh, northern iran, Engineering Applications of Computational Fluid Mechanics 12 (2018) 724–737.

[126] M. Ehteram, F. B. Othman, Z. M. Yaseen, H. A. Afan, M. F. Allawi, M. B. A. Malek, A. N. Ahmed, S. Shahid, V. P. Singh, A. El-Shafie, Improving the muskingum flood routing method using a hybrid of particle swarm optimization and bat algorithm, Water 10 (2018) 807.

[127] E. Camci, D. R. Kripalani, L. Ma, E. Kayacan, M. A. Khanesar, An aerial robot for rice farm quality inspection with type-2 fuzzy neural networks tuned by particle swarm optimization-sliding mode control hybrid algorithm, Swarm and Evolutionary Computation 41 (2018) 1–8.

[128] L. M. Maiyar, J. J. Thakkar, Environmentally conscious logistics planning for food grain industry considering wastages employing multi objective hybrid particle swarm optimization, Transportation Research Part E: Logistics and Transportation Review 127 (2019) 220–248.

[129] A. A. Alnaqi, H. Moayedi, A. Shahsavar, T. K. Nguyen, Prediction of energetic performance of a building integrated photovoltaic/thermal system thorough artificial neural network and hybrid particle swarm optimization models, Energy Conversion and Management 183 (2019) 137–148.

[130] A. Mohebbi, S. Achiche, L. Baron, Integrated and concurrent detailed design of a mechatronic quadrotor system using a fuzzy-based particle swarm optimization, Engineering Applications of Artificial Intelligence 82 (2019) 192–206.

[131] H. Wang, M. jun Peng, J. W. Hines, G. yang Zheng, Y. kuo Liu, B. R. Upadhyaya, A hybrid fault diagnosis methodology with support vector machine and improved particle swarm optimization for nuclear power plants, ISA Transactions 95 (2019) 358–371.

[132] G. Liu, W. Chen, H. Chen, Quantum particle swarm with teamwork evolutionary strategy for multi-objective optimization on electro-optical platform, IEEE Access 7 (2019) 41205–41219.

[133] H. Jiang, C. K. Kwong, W. Y. Park, K. M. Yu, A multi-objective pso approach of mining association rules for affective design based on online customer reviews, Journal of Engineering Design 29 (2018) 381–403.

[134] M. Song, K. Chen, J. Wang, Three-dimensional wind turbine positioning using gaussian particle swarm optimization with differential evolution, Journal of Wind Engineering and Industrial Aerodynamics 172 (2018) 317–324.

[135] N. H. A. Rahman, A. F. Zobaa, Integrated mutation strategy with modified binary pso algorithm for optimal pmus placement, IEEE Transactions on Industrial Informatics 13 (2017) 3124–3133.

[136] Y. Jin, B. Sendhoff, A systems approach to evolutionary multiobjective structural optimization and beyond, IEEE Computational Intelligence Magazine 4 (2009) 62–76.

[137] B. qiu Tang, J. Han, G. feng Guo, Y. Chen, S. Zhang, Building material prices forecasting based on least square support vector machine and improved particle swarm optimization, Architectural Engineering and Design Management 15 (2019) 196–212.

[138] J. Shen, L. Han, Design process optimization and profit calculation module development simulation analysis of financial accounting information system based on particle swarm optimization (pso)(retraction of vol 18, pg 809, 2020) (2022).

[139] Intelligent prediction of transmission line project cost based on least squares support vector machine optimized by particle swarm optimization, Mathematical Problems in Engineering 2018 (2018) 1–11.

[140] D. Pradeepkumar, V. Ravi, Forecasting financial time series volatility using particle swarm optimization trained quantile regression neural network, Applied Soft Computing 58 (2017) 35–52.

[141] S. Abid, A. Zafar, R. Khalid, S. Javaid, U. Qasim, Z. A. Khan, N. Javaid, Managing energy in smart homes using binary particle swarm optimization, in: Complex, Intelligent, and Software Intensive Systems: Proceedings of the 11th International Conference on Complex, Intelligent, and Software Intensive Systems (CISIS-2017), Springer, 2018, pp. 189–196.

[142] L. Li, L. Qin, X. Qu, J. Zhang, Y. Wang, B. Ran, Day-ahead traffic flow forecasting based on a deep belief network optimized by the multi-objective particle swarm algorithm, Knowledge-Based Systems 172 (2019) 1–14.

[143] A. R. Jordehi, Binary particle swarm optimisation with quadratic transfer function: A new binary optimisation algorithm for optimal scheduling of appliances in smart homes, Applied Soft Computing 78 (2019) 465–480.

[144] L. T. Le, H. Nguyen, J. Zhou, J. Dou, H. Moayedi, Estimating the heating load of buildings for smart city planning using a novel artificial intelligence technique pso-xgboost, Applied Sciences 9 (2019) 2714.

[145] K. Ma, S. Hu, J. Yang, X. Xu, X. Guan, Appliances scheduling via cooperative multi-swarm pso under day-ahead prices and photovoltaic generation, Applied Soft Computing 62 (2018) 504–513.

[146] W. Hu, H. Wang, Z. Qiu, C. Nie, L. Yan, A quantum particle swarm optimization driven urban traffic light scheduling model, Neural Computing and Applications 29 (2018) 901–911.

[147] M. Sato, Y. Fukuyama, T. Iizaka, T. Matsui, Total optimization of energy networks in a smart city by multi-swarm differential evolutionary particle swarm optimization, IEEE Transactions on Sustainable Energy 10 (2019) 2186–2200.

[148] S. T. Ramya, B. Arunagiri, P. Rangarajan, Novel effective x-path particle swarm optimization based deprived video data retrieval for smart city, Cluster Computing 22 (2019) 13085–13094.

[149] A. Bhattacharya, R. T. Goswami, K. Mukherjee, A feature selection technique based on rough set and improvised pso algorithm (psors-fs) for permission based detection of android malwares, International Journal of Machine Learning and Cybernetics 10 (2019) 1893–1907.

[150] R. Zarrouk, I. E. Bennour, A. Jemai, A two-level particle swarm optimization algorithm for the flexible job shop scheduling problem, Swarm Intelligence 13 (2019) 145–168.

[151] M. Nouiri, A. Bekrar, A. Jemai, S. Niar, A. C. Ammari, An effective and distributed particle swarm optimization algorithm for flexible job-shop scheduling problem, Journal of Intelligent Manufacturing 29 (2018) 603–615.

[152] N. Mansouri, B. M. H. Zade, M. M. Javidi, Hybrid task scheduling strategy for cloud computing by modified particle swarm optimization and fuzzy theory, Computers Industrial Engineering 130 (2019) 597–633.

[153] Y. Zhong, J. Lin, L. Wang, H. Zhang, Discrete comprehensive learning particle swarm optimization algorithm with metropolis acceptance criterion for traveling salesman problem, Swarm and Evolutionary Computation 42 (2018) 77–88.

[154] S. Thabit, A. Mohades, Multi-robot path planning based on multi-objective particle swarm optimization, IEEE Access 7 (2019) 2138–2147.

[155] R. Sivaranjani, S. M. M. Roomi, M. Senthilarasi, Speckle noise removal in sar images using multi-objective pso (mopso) algorithm, Applied Soft Computing 76 (2019) 671–681.

[156] G. Lin, J. Guan, Z. Li, H. Feng, A hybrid binary particle swarm optimization with tabu search for the set-union knapsack problem, Expert Systems with Applications 135 (2019) 201–211.

[157] Z. Sun, Y. Liu, L. Tao, Attack localization task allocation in wireless sensor networks based on multi-objective binary particle swarm optimization, Journal of Network and Computer Applications 112 (2018) 29–40.

[158] M. Alswaitti, M. Albughdadi, N. A. M. Isa, Density-based particle swarm optimization algorithm for data clustering, Expert Systems with Applications 91 (2018) 170–186.

[159] S. Suresh, S. Lal, Multilevel thresholding based on chaotic darwinian particle swarm optimization for segmentation of satellite images, Applied Soft Computing 55 (2017) 503–522.

[160] F. Sheikholeslami, N. J. Navimipour, Service allocation in the cloud environments using multi-objective particle swarm optimization algorithm based on crowding distance, Swarm and Evolutionary Computation 35 (2017) 53–64.

[161] F. Liu, H. Huang, X. Li, Z. Hao, Automated test data generation based on particle swarm optimisation with convergence speed controller, CAAI Transactions on Intelligence Technology 2 (2017) 73–79.

[162] S. Gu, R. Cheng, Y. Jin, Feature selection for high-dimensional classification using a competitive swarm optimizer, Soft Computing 22 (2018) 811–822.

[163] J. Li, J. Zhang, C. Jiang, M. Zhou, Composite particle swarm optimizer with historical memory for function optimization, IEEE Transactions on Cybernetics 45 (2015) 2350–2363.

[164] Q. Liu, W. Wei, H. Yuan, Z.-H. Zhan, Y. Li, Topology selection for particle swarm optimization, Information Sciences 363 (2016) 154–173.

[165] J. Aberbour, M. Graba, A. Kheldoun, Effect of cost function and pso topology selection on the optimum design of pid parameters for the avr system, in: 2015 4th International Conference on Electrical Engineering (ICEE), IEEE, 2015, pp. 1–5.

[166] J. K. Proud, D. T. Lai, K. L. Mudie, G. L. Carstairs, D. C. Billing, A. Garofolini, R. K. Begg, Exoskeleton application to military manual handling tasks, Human Factors 64 (3) (2022) 527–554.

[167] P. Yuan, T. Wang, F. Ma, M. Gong, Key technologies and prospects of individual combat exoskeleton, in: Knowledge Engineering and Management, Springer, 2014, pp. 305–316.

[168] M. R. Islam, M. Rahmani, M. H. Rahman, A novel exoskeleton with fractional sliding mode control for upper limb rehabilitation, Robotica 38 (11) (2020) 2099–2120.

[169] Q. Wu, X. Wang, B. Chen, H. Wu, Development of an rbfn-based neural-fuzzy adaptive control strategy for an upper limb rehabilitation exoskeleton, Mechatronics 53 (2018) 85–94.

[170] B. Achili, T. Madani, B. Daachi, K. Djouani, Adaptive observer based on mlpnn and sliding mode for wearable robots: application to an active joint orthosis, Neurocomputing 197 (2016) 69–77.

[171] X. Huang, F. Naghdy, H. Du, G. Naghdy, C. Todd, Reinforcement learning neural network (rlnn) based adaptive control of fine hand motion rehabilitation robot, in: 2015 IEEE Conference on Control Applications (CCA), IEEE, 2015, pp. 941–946.

[172] W. He, S. S. Ge, Y. Li, E. Chew, Y. S. Ng, Neural network control of a rehabilitation robot by state and output feedback, Journal of Intelligent & Robotic Systems 80 (1) (2015) 15–31.

[173] A. Belkadi, H. Oulhadj, Y. Touati, S. A. Khan, B. Daachi, On the robust pid adaptive controller for exoskeletons: A particle swarm optimization based approach, Applied Soft Computing 60 (2017) 87–100.

[174] S. Chacko, C. N. Bhende, S. Jain, R. K. Nema, Pso based online tuning of pi controller for estimation of rotor resistance of indirect vector controlled induction motor drive, in: 2016 International Conference on Electrical, Electronics, and Optimization Techniques (ICEEOT), IEEE, 2016, pp. 4606–4611.

[175] P.-L. Chen, M.-C. Yang, T.-Y. Sun, Pso-based on-line tuning pid controller for setpoint changes and load disturbance, in: 2011 IEEE Congress of Evolutionary Computation (CEC), IEEE, 2011, pp. 1887–1894.

[176] V. Khoshdel, A. Akbarzadeh, N. Naghavi, A. Sharifnezhad, M. Souzanchi-Kashani, semg-based impedance control for lower-limb rehabilitation robot, Intelligent Service Robotics 11 (1) (2018) 97–108.

[177] T. Teramae, T. Noda, J. Morimoto, Emg-based model predictive control for physical human–robot interaction: Application for assist-as-needed control, IEEE Robotics and Automation Letters 3 (1) (2017) 210–217.

[178] Z. Li, B. Wang, F. Sun, C. Yang, Q. Xie, W. Zhang, semg-based joint force control for an upper-limb power-assist exoskeleton robot, IEEE journal of biomedical and health informatics 18 (3) (2013) 1043–1050.

[179] H. Su, Z. Li, G. Li, C. Yang, Emg-based neural network control of an upper-limb power-assist exoskeleton robot, in: International Symposium on Neural Networks, Springer, 2013, pp. 204–211.

[180] B.-C. Tsai, W.-W. Wang, L.-C. Hsu, L.-C. Fu, J.-S. Lai, An articulated rehabilitation robot for upper limb physiotherapy and training, in: 2010 IEEE/RSJ International Conference on Intelligent Robots and Systems, IEEE, 2010, pp. 1470–1475.

[181] H. Tiaiba, M. E. H. Daachi, T. Madani, Real-time adaptive super twisting algorithm based on pso algorithm: Application for an exoskeleton robot, Robotica (2024) 1–26.

[182] S. Jian, L. Zhitao, S. Hongye, A second-order sliding mode control design for bidirectional dcdc converter, in: 2017 36th Chinese Control Conference (CCC), IEEE, 2017, pp. 9181–9186.

[183] H. Imine, L. M. Fridman, T. Madani, Steering control for rollover avoidance of heavy vehicles, IEEE Transactions on Vehicular Technology 61 (8) (2012) 3499–3509.

[184] T. L. Dang, Y. Hoshino, Improved pso algorithm for training of neural network in co-design architecture, International Journal of Computer Applications 975 (2019) 8887.

[185] J. A. Moreno, A linear framework for the robust stability analysis of a generalized super-twisting algorithm, in: 2009 6th International Conference on Electrical Engineering, Computing Science and Automatic Control (CCE), IEEE, 2009, pp. 1–6.

[186] J. A. Moreno, M. Osorio, A lyapunov approach to second-order sliding mode controllers and observers, in: 2008 47th IEEE conference on decision and control, IEEE, 2008, pp. 2856–2861.

[187] S. Boyd, L. El Ghaoui, E. Feron, V. Balakrishnan, Linear matrix inequalities in system and control theory, SIAM, 1994.